Coupled-cluster approximation for spin lattices: Application to solid ^{3}He

M. Roger
Service de Physique du Solide et de Résonance Magnétique, Commissariat à l'Energie Atomique, Orme des Merisiers, 91191 Gif-sur-Yvette CEDEX, France

J. H. Hetherington
Department of Physics and Astronomy, Michigan State University, East Lansing, Michigan 48824
(Received 10 May 1989)

We have extended the coupled-cluster approximation to the spin-lattice problem. The efficiency of this method is demonstrated on simple antiferromagnetic Heisenberg models in one and two dimensions. We then apply it to the problem of the ground state of the spins of solid ^{3}He in the presence of multiple spin exchanges. The first-order transition field between the two ordered phases is calculated, using the exchange parameters determined from first principles. Its variations as a function of the molar volume are predicted.

I. INTRODUCTION

The coupled-cluster approximation (CCA) has been developed mainly for application to systems of fermions (e.g., nuclear matter). It has proved to be very useful in quantum chemistry where very accurate energies are required to explain chemical phenomena. The theory has gradually been taken over into other areas of physics where accuracy beyond that provided by Hartree or Hartree-Fock variational wave functions is needed. An excellent, although not very detailed review[1] provided us with the stimulation to apply the method to spin-lattice systems. As far as we know, the method has not been applied to such systems despite the long history of attempts to improve on available methods for those problems.

The lattice problem we had in mind was the spin Hamiltonian of bcc ^{3}He. This Hamiltonian is now known to contain several types of exchange including two-spin exchange and three-spin exchange, which lead to Heisenberg-type terms, and four-spin and six-spin ring exchanges which lead to σ^4- and σ^6-type terms.[2-6] Until now the ground state of this problem has only been studied in mean-field theory[3,7,8] or by exact diagonalization of the 16-atom cluster,[9] and somewhat tentatively by the random-phase approximation.[3,10,11]

The coupled-cluster method starts with a variational ground state $|0\rangle$ (which is provided by mean-field theory in the case of the spin lattice) and develops a better (although unnormalized) approximation in the form $e^S|0\rangle$. The operator S contains only raising operators (in the case of spins, flipping them out of the ground-state direction) and is usually treated in approximations denoted by how many particles are raised by a single operation of S as SUB2, SUB3, etc.[1]

$$S = S_2 + S_3 + S_4 + \cdots . \tag{1}$$

The method is manifestly convergent towards the exact result as more terms in S are included. Even though it will not be possible to go very far in this process because of the computational effort required, it is in contrast to the random-phase approximation (RPA), for example, where one does not know a good next approximation even in principle. Note that in Eq. (1) we have omitted the S_1 term reflecting the fact that operators that raise a single particle are equivalent to changes in the variational wave function. For the spin-lattice problem we find that the strict breakdown into SUBn is not very useful, since some effects at SUB4 are substantially larger than certain effects at SUB2; it is better to keep all reasonable terms inside a compact cluster than to include SUB2 terms where the two spins are far apart.

In the next section we introduce the method in a form suitable for application to spin-lattice Hamiltonians of a rather general form. In Sec. III we provide several examples of application to simple problems for which the exact or near exact result is known. These simple examples are useful pedagogically and also provide an insight to the accuracy to be expected from the method. In Sec. IV we study the multiple exchange Hamiltonian first on a square lattice then on the bcc lattice with realistic exchange parameters. This last problem formed the motivation for the transportation of the CCA method to spin lattices. In ^{3}He a number of spin ring exchanges are important in the order 2, 4 planar, 3, 6 hexagonal, 4 folded, etc., as suggested by analytic approximations[5] and more quantitatively by Monte Carlo calculations.[6] Thus we have included terms up to SUB4 inside a planar cluster of four spins, which treats the first three kinds of exchange rather completely and have made corrections to take account of the relatively smaller six-spin term in the Hamiltonian. In the future it may be possible to treat consistently a larger cluster including the six-spin exchange.

II. THE COUPLED-CLUSTER METHOD ON SPIN SYSTEMS

We will consider a lattice of N spin-$\frac{1}{2}$ sites. These spins will interact through a Hamiltonian of the form

$$\mathcal{H}=\sum_{P_2}\sum_{i<j}^{(P_2)}F_{\alpha\beta}^{(P_2)}\sigma_i^\alpha\sigma_j^\beta + \sum_{P_4}\sum_{i<j<k<l}^{(P_4)}F_{\alpha\beta\gamma\delta}^{(P_4)}\sigma_i^\alpha\sigma_j^\beta\sigma_k^\gamma\sigma_l^\delta+\cdots-B\sum_i\sigma_i^z\ , \tag{2}$$

where B is the magnetic field times the magnetic moment $\gamma\hbar/2$, the F's indicate the kind and strength of the coupling, P_n indicates the kind of cycle or panel of spins in the interaction of n spins, the greek indices run over spin directions (x,y,z) and are summed as implied by their being repeated, and the latin indices run over the N spins (with restrictions indicated by the panel P and the inequalities on the summation). We have assumed, as is usual, that the σ's refer to directions in the Zeeman basis, that is with σ_z along the direction of the magnetic field. As examples, ordinary Heisenberg coupling will result if F is of the form

$$F_{\alpha\beta}=J\delta_{\alpha\beta}\ ,$$

while the four-σ part of the four-spin ring exchange Hamiltonian is of the form

$$F_{\alpha\beta\gamma\delta}=K(\delta_{\alpha\beta}\delta_{\gamma\delta}+\delta_{\beta\gamma}\delta_{\alpha\delta}-\delta_{\alpha\gamma}\delta_{\beta\delta})\ .$$

The panels P_2 imply a summation restriction over certain kinds of pairs for example nearest neighbors, next-nearest neighbors, etc. The panels P_4 would run over planar quadrilaterals with nearest-neighbor sides, folded quadrilaterals of nearest neighbors, etc. We have not included P_3 because combinations of three spins violate time reversal and do not appear as a result of spin permutations (although strange magnetic interactions could lead to three-σ terms).

As mentioned in the Introduction, the transformation of the basis to one where the state $|0\rangle$ is a variational minimum is an important step in the application of the coupled-cluster method. The mean-field approximation is equivalent to the Hartree minimization in that the state constructed is a product of single-particle wave functions (spinors in our case), which gives minimum expectation value of the Hamiltonian. The local mean fields give a direction for each spin's coordinate system and we can build a basis where the 2^N states are specified by which spins are flipped from their mean-field direction. Introducing the set of 2×2 rotation matrices U_i that rotate the coordinate system of the ith spin from the Zeeman (magnetic field) basis to the Néel (mean-field) basis the Hamiltonian becomes

$$H=\sum_{P_2}\sum_{i<j}^{(P_2)}F_{\alpha\beta}^{(P_2)}(U_i\sigma_i^\alpha U_i^\dagger)(U_j\sigma_j^\beta U_j^\dagger)+\cdots-B\sum_i(U_i\sigma_i^zU_i^\dagger)\ . \tag{3}$$

Each factor $U\sigma U^\dagger$ represents a traceless 2×2 matrix and can be written in terms of the three matrices $\sigma^x,\sigma^y,\sigma^z$ or, as is a more convenient form for our purposes,

$$\sigma^+=(\sigma^x+i\sigma^y)/2,\quad \sigma^-=(\sigma^x-i\sigma^y)/2,\quad \sigma^z\ . \tag{4}$$

Thus if we write

$$U_i\sigma_i^\alpha U_i^\dagger=C_\rho^\alpha(i)\sigma_i^\rho\ , \tag{5}$$

where ρ is summed over $+,-,z$, and by defining

$$B_\rho(i)=BC_\rho^z(i)\ , \tag{6}$$

$$G_{\rho\tau}^{(P_2)}(i,j)=F_{\alpha\beta}^{(P_2)}C_\rho^\alpha(i)C_\tau^\beta(j)\ , \tag{7}$$

etc., we have for the Hamiltonian in terms of raising, lowering, and σ^z operators in the mean-field basis,

$$H=\sum_{P_2}\sum_{i<j}^{(P_2)}G_{\rho\tau}^{(P_2)}(i,j)\sigma_i^\rho\sigma_j^\tau+\sum_{P_4}\sum_{i<j}^{(P_4)}G_{\rho\tau\mu\nu}^{(P_4)}(i,j,k,l)\sigma_i^\rho\sigma_j^\tau\sigma_k^\mu\sigma_l^\nu+\cdots-\sum_i B_\rho(i)\sigma_i^\rho\ . \tag{8}$$

This Hamiltonian forms the convenient starting place for the application of the CCA. In all cases we have studied, it has been convenient to choose the matrix U so that the rotations are about the y axis, which keeps the expression for the Hamiltonian real. We have also taken the convention that states $|0\rangle$ has all spins "down" (i.e., $\sigma^-|0\rangle=0$). Besides being a "best" starting place because the state $|0\rangle$ in this basis is the mean-field (i.e., variational in a Fock space) ground state, the Hamiltonian (8) has zero matrix elements between $|0\rangle$ and any state with a single spin flipped. This can be seen from the fact that variation of a given spin direction is essentially the same as adding some of the flipped state. Algebraically

$$\langle0|\sigma_i^-H|0\rangle=\left\langle0\left|\left[2\frac{\partial U_i}{\partial\theta_i}\left[\prod_{j\neq i}U_j\right]\mathcal{H}\left[\prod_k U_k^\dagger\right]\right]\right|0\right\rangle=\frac{\partial}{\partial\theta_i}\langle0|H|0\rangle\ . \tag{9}$$

Here we have assumed $U^\dagger=\exp(i\theta\sigma^y/2)$. The last member is zero because θ is chosen to minimize the expectation value of the energy.

One of the characteristics of the CCA method is that it yields an unnormalized ground state. This prevents our being able to prove a variational theorem but results in terminating series and more tractable solutions. The CCA ground state is taken to be

$$|\Phi\rangle=e^S|0\rangle\ , \tag{10}$$

where

$$S=\sum_{P_2}\sum_{i<j}^{(P_2)}\chi_{ij}\sigma_i^+\sigma_j^+ + \sum_{P_3}\sum_{i<j<k}^{(P_3)}\tau_{ijk}\sigma_i^+\sigma_j^+\sigma_k^+ + \sum_{P_4}\sum_{i<j<k<l}^{(P_4)}\kappa_{ijkl}\sigma_i^+\sigma_j^+\sigma_k^+\sigma_l^+ +\cdots\ , \tag{11}$$

where successive terms are denoted SUB2, SUB3, SUB4,

etc. As mentioned earlier we can omit S_1 terms because these are equivalent to changes in the mean-field basis.

The commutation relations among the operators we are using are

$$[\sigma_i^\rho,\sigma_j^\tau]=0 \quad \text{if } i\neq j \quad \text{or if } \rho=\tau\ , \tag{12}$$

$$[\sigma_i^-,\sigma_i^+]=-\sigma_i^z\ , \tag{13a}$$

$$[\sigma_i^z,\sigma_i^+]=2\sigma_i^+\ , \tag{13b}$$

$$[\sigma_i^z,\sigma_i^-]=-2\sigma_i^-\ . \tag{13c}$$

We also have

$$(\sigma_i^+)^2=0=(\sigma_i^-)^2\ , \tag{14}$$

$$\sigma_i^+\sigma_i^-+\sigma_i^-\sigma_i^+=1\ . \tag{15}$$

The formal statement of the CCA method is as follows: Assume that the (unnormalized) ground state of the system is of the form

$$|\Phi\rangle=e^S|0\rangle\ , \tag{16}$$

which is always possible[1] if $|\Phi\rangle$ is not exactly orthogonal to $|0\rangle$. Then

$$H|\Phi\rangle=E_0|\Phi\rangle \tag{17}$$

or

$$He^S|0\rangle=E_0e^S|0\rangle\ . \tag{18}$$

Multiplying on the left by e^{-S} one has

$$\tilde{H}|0\rangle\equiv e^{-S}He^S|0\rangle=E_0|0\rangle\ . \tag{19}$$

Now since $|0\rangle$ is normalized we may write

$$\langle 0|\tilde{H}|0\rangle=\langle 0|e^{-S}He^S|0\rangle=E_0\ , \tag{20}$$

and by the orthogonality of $|n\rangle,|0\rangle$, where $|n\rangle$ are excited states of the mean-field basis

$$\langle n|\tilde{H}|0\rangle=\langle n|e^{-S}He^S|0\rangle=0\ . \tag{21}$$

Equations (21) are the requirements on S so that (20) will be true. In fact, there are more Eqs. (21) than parameters in S to be adjusted, but in practice if the lower states' equations are satisfied the energy given by (20) is a good approximation. One attractive feature of the method is that there is a clear succession of approximations (SUB2, SUB3, etc., for example) that leads to the exact ground state.

An important point, which leads to finiteness of the equations, is that $\tilde{H}$ is a closed expression for any finite level of approximation. First note that

$$\tilde{H}=e^{-S}He^S=H+[H,S]+\frac{1}{2!}[[H,S],S]+\cdots\ , \tag{22}$$

and, since S contains only σ^+'s and H contains only a finite product of σ's, each successive commutation with S reduces the operators in the progression

$$\sigma^-\rightarrow\sigma^z\rightarrow\sigma^+\rightarrow 0 \tag{23}$$

so that the series (22) is always finite for H's with a finite number of σ's in each term.

In practice, we shall proceed in the following way. We use the property

$$\exp(-S)\sigma_i^\rho\sigma_j^\tau\sigma_k^\mu\sigma_l^\gamma\cdots\exp(S)=\tilde{\sigma}_i^{\,\rho}\tilde{\sigma}_j^{\,\tau}\tilde{\sigma}_k^{\,\mu}\tilde{\sigma}_l^{\,\gamma}\cdots \tag{24}$$

with

$$\tilde{\sigma}_i^{\,\lambda}=\exp(-S)\sigma_i^\lambda\exp(S)=\sigma_i^\lambda+[\sigma_i^\lambda,S]+\frac{1}{2!}[[\sigma_i^\lambda,S],S]\ . \tag{25}$$

All that we now need are the $\exp(S)$ transforms of the three operators: $\sigma_i^+,\sigma_i^-,\sigma_i^z$. From Eq. (25) we obtain

$$\tilde{\sigma}_i^{\,+}=\sigma_i^+\ , \tag{26a}$$

$$\tilde{\sigma}_i^{\,-}=\sigma_i^-+[\sigma_i^-,\sigma_i^+]\mathcal{S}_i-\sigma_i^+\mathcal{S}_i^2\ , \tag{26b}$$

$$\tilde{\sigma}_i^{\,z}=[\sigma_i^+,\sigma_i^-]+2\sigma_i^+\mathcal{S}_i\ , \tag{26c}$$

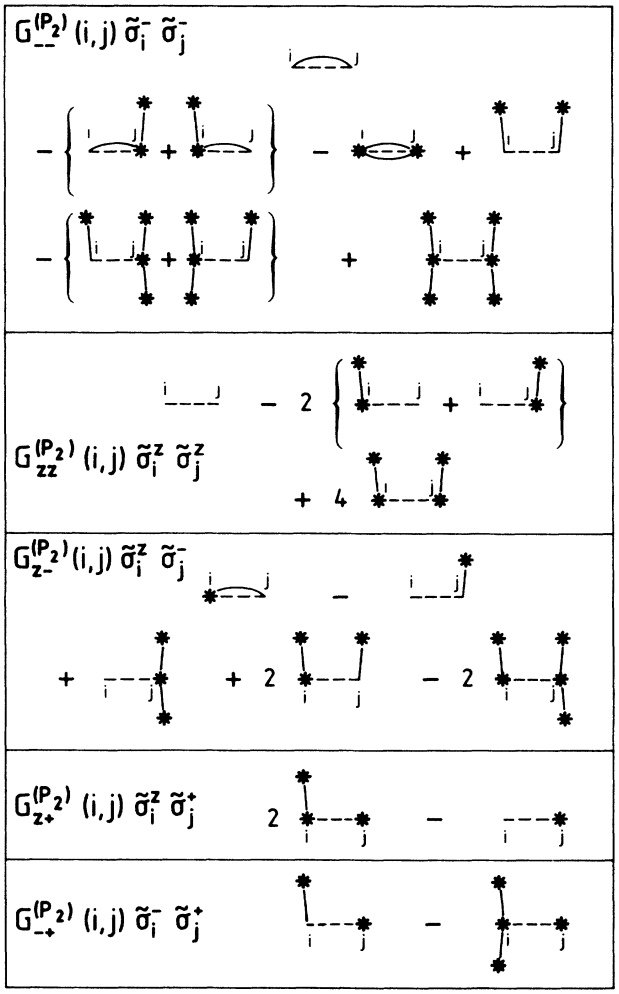

FIG. 1. A diagrammatic representation of the different terms contributing to $\tilde{H}|0\rangle$ for a quadratic Hamiltonian, within the "SUB2 coupled-cluster approximation." A dashed line represents a link $G^{(P_2)}_{\rho\tau}(i,j)$ in the general expression (8) of the Hamiltonian. A solid line represents a pair-flip amplitude χ_{kl} in Eq. (11). A star (*) represents a creation operator σ_k^+. These diagrams are to be summed over a given lattice with the convention that all ends remain free.

where $\sigma_i^+ \mathcal{S}_i$ represents the sum of all terms of S that are connected to the site i (i.e., which contain σ_i^+).

$$\mathcal{S}_i = \sum_{P_2^i} \sum_{j}^{(P_2^i)} \chi_{ij}\sigma_j^+ + \sum_{P_3^i} \sum_{j<k}^{(P_3^i)} \tau_{ijk}\sigma_j^+\sigma_k^+ + \sum_{P_4^i} \sum_{j<k<l}^{(P_4^i)} \kappa_{ijkl}\sigma_j^+\sigma_k^+\sigma_l^+ + \cdots . \tag{27}$$

The sums over P_n^i are over those panels that include the site i. The sums over $j,k,l,\ldots$ are restricted to the panels P_n^i. In Eqs. (26) we have written σ^z as $[\sigma^+,\sigma^-]$ to emphasize that it is often convenient in automatic calculations to have fewer kinds of operators.

The expression of $\tilde{H}$ is obtained by substituting the relations (26a)–(26c) into (8). In fact, we only need $\tilde{H}|0\rangle$, and this is the more convenient form: Using the relation (15) we can move all σ_l^- to the right, and, since $\sigma_l^-|0\rangle=0$, we are left with operator products that contain exclusively raising operators σ_p^+.

The calculation is straightforward with a quadratic Hamiltonian. We simply have to calculate the following terms: $\tilde{\sigma}_i^{\rho}\tilde{\sigma}_j^{\tau}$, with $\rho,\tau\in\{+,-,z\}$. The results are conveniently represented by the diagrams of Fig. 1 when S is terminated at the SUB2 level, so that only the first term is retained in Eq. (27). We use the following conventions: A dashed line represents a $G_{\rho\tau}^{(P_2)}(i,j)$ link in the Hamiltonian (8). A solid line represents a χ_{ij} link in the expression for $\mathcal{S}$ [relation (27)]. The stars ($*$) represent σ_k^+ operators. The coefficient of terms in the expression for $\tilde{H}|0\rangle$ that have a given arrangement on the lattice of σ^+'s is given by the sum over diagrams that have their $*$'s so arranged. Each diagram is weighted by $G_{\rho\tau}^{(P_2)}(i,j)$ for the single dotted line and by χ_{km} for each solid line and by the coefficient leading the diagram in Fig. 1.

Because of our interest in ^{3}He magnetism (see Sec. III) a computer program has been written (see the Appendix) for treating more complicated Hamiltonians, which include σ^4 terms. Its automatically performs the $\tilde{\sigma}_i^{\rho}$ products, reduces them with the help of Eq. (15) and sums over a given lattice. The resulting set of nonlinear coupled equations (21) is usually solved by the Newton-Raphson method.[12]

III. THE ILLUSTRATION OF THE METHOD ON SIMPLE MODELS

In this section we present three simple examples demonstrating the applicability and accuracy of the coupled-cluster method on spin-lattice Hamiltonians. The first one is pedagogic: The concepts introduced in Sec. II are illustrated on the Heisenberg antiferromagnet in one and two dimensions (square lattice). Secondly, we show that the method works as well in the presence of a an arbitrary magnetic field B. Finally, since our objective is to apply the method to a frustrated Hamiltonian with competing interactions (the physical situation[2–6] in solid ^{3}He), we study the Heisenberg linear chain with frustrated antiferromagnetic interactions between first and second neighbors. In all cases, comparison is made with exact results and/or other approximations.

A. The Heisenberg antiferromagnet in one and two dimensions

1. The antiferromagnetic Heisenberg linear chain

Here in the usual notation the Hamiltonian is simply

$$H=\frac{J}{2}\sum_{i=1}^{N}\boldsymbol{\sigma}_i\cdot\boldsymbol{\sigma}_{i+1} . \tag{28}$$

This can be transformed into the mean-field (or rather Néel) basis

$$H=-\frac{J}{2}\sum_{i=1}^{N}[2(\sigma_i^+\sigma_{i+1}^+ + \sigma_i^-\sigma_{i+1}^-)+\sigma_i^z\sigma_{i+1}^z] . \tag{29}$$

In this basis the two degenerate Néel states correspond to all spins "down" (in their individual coordinate systems) or all spins "up." We arbitrarily choose the "down" state as our starting state $|0\rangle$.

Assume S to allow flipping a nearest-neighbor pair, which is to say in the Néel basis that neighboring pairs are raised. Note that this is not the whole SUB2 approximation usually discussed but is only a subset of possible two spin excitations

$$S=\sum_i \chi_1\sigma_i^+\sigma_{i+1}^+ . \tag{30}$$

From Eq. (24), the transformed Hamiltonian becomes simply

$$\tilde{H}=e^{-S}He^{S}=-\frac{J}{2}\sum_{i=1}^{N}[2(\tilde{\sigma}_i^+\tilde{\sigma}_{i+1}^+ + \tilde{\sigma}_i^-\tilde{\sigma}_{i+1}^- + \tilde{\sigma}_i^z\tilde{\sigma}_{i+1}^z] . \tag{31}$$

Using the diagrams of Fig. 1, we have

$$\tilde{H}|0\rangle=-\frac{J}{2}\sum_i[(1+2\chi_1)|0\rangle+(2-4\chi_1-6\chi_1^2)\sigma_i^+\sigma_{i+1}^+|0\rangle + (2\chi_1^2)\sigma_i^+\sigma_{i+3}^+|0\rangle+(4\chi_1^2)\sigma_i^+\sigma_{i+1}^+\sigma_{i+2}^+\sigma_{i+3}^+|0\rangle] . \tag{32}$$

The parameter χ_1 is determined by setting the second term in Eq. (32) to zero so that $\tilde{H}$ is diagonal in the space of $|0\rangle$ and all states with two nearest neighbors flipped. Thus

$$0=2-4\chi_1-6\chi_1^2 \quad \text{or} \quad \chi_1=\tfrac{1}{3} . \tag{33}$$

The ground-state energy is then

$$E_0/NJ=\langle 0|\tilde{H}|0\rangle/NJ = -(1+2\chi_1)/2=-0.8333\ldots . \tag{34}$$

Table I shows how this compares with mean field, spin waves,[13] and the exact result.[14]

We also compare with the result obtained with the variational "resonant-valence-bond" (RVB) wave function (in its simplest formulation) proposed by Ander-

TABLE I. Ground-state energies of the antiferromagnetic Heisenberg linear chain (first line) and of the antiferromagnetic Heisenberg model on a two-dimensional square lattice (second line). The energies within a scheme of successive "coupled-cluster approximations" with increasing cluster size (CCA1, CCA2,. . .) are compared to the mean-field (MF), spin-wave,[13] RVB variational[15] and exact[14] or nearly exact[16] results.

	MF	RVB	Spin waves	CCA1	CCA2	≈exact
One dimensional	0.5	0.750	0.865	0.8333	0.8725	0.8863
Two dimensional	1.0		1.316	1.297	1.306	1.33

son.[15] It is worth noticing that the exp(S) formalism that we are developing contains the RVB wave function as a particular case. If we split the chain into odd and even bonds and take

$$S=\sum_i \chi_e \sigma_{2i}^+ \sigma_{2i+1}^+ + \chi_0 \sigma_{2i-1}^+ \sigma_{2i}^+ \tag{35}$$

with $\chi_e=1$ and $\chi_0=0$, we obtain

$$\exp(S)|0\rangle = \prod_i (1+\sigma_{2i}^+ \sigma_{2i+1}^+)|0\rangle \ , \tag{36}$$

which simply represents the RVB wave function [we use the properties that all σ_i^+ commute and $(\sigma_i^+)^2=0$]. However, by applying the same formalism with Eq. (35), the equation (33) is replaced by the system

$$\begin{aligned} 0&=1-2\chi_e-2\chi_e\chi_0-\chi_e^2 \ , \\ 0&=1-2\chi_0-2\chi_e\chi_0-\chi_0^2 \ , \end{aligned} \tag{37}$$

which gives back the symmetric solution $\chi_e=\chi_0=\frac{1}{3}$ as we previously assumed. Of course, the result $\chi_e=\chi_0$ is not exactly contrary to the spirit of the RVB idea although the bonds are not "saturated" as is often assumed.

Note that the third and fourth terms in Eq. (32) are not actually zero in the preceding approximations. The next logical level of approximation is suggested, however: include in S terms that flip third-neighbor pairs and terms that flip four first neighbors as found in the third and fourth terms of Eq. (32). This will allow cancellation of terms of that type (and creation of other remainder terms presumably of a still smaller size). Thus a logical sequence of approximations for lattice spin systems is to include at the first level creation operator that are in the Hamiltonian, which connects the ground state to other states in the mean-field basis. At the second level include in addition those terms that are remainders in $\tilde{H}|0\rangle$ at the first level, etc. In other words, if we take S_n to include remainder terms from $\tilde{H}_{n-1}|0\rangle$ (where $\tilde{H}_0$ is the starting Hamiltonian in the mean-field basis), then we have a succession of approximations that will eventually converge to the exact result. Thus at the next approximation we take

$$S=\sum_i (\chi_1 \sigma_i^+ \sigma_{i+1}^+ + \chi_3 \sigma_i^+ \sigma_{i+3}^+ + \kappa \sigma_i^+ \sigma_{i+1}^+ \sigma_{i+2}^+ \sigma_{i+3}^+) \ . \tag{38}$$

When this is carried out for the linear chain, we obtain

$$\begin{aligned} \tilde{H}|0\rangle = -\frac{J}{2}\sum_i \{&(1+2\chi_1)|0\rangle + (2-4\chi_1-6\chi_1^2+4\chi_1\chi_3+4\chi_3^2+4\kappa)\sigma_i^+\sigma_{i+1}^+|0\rangle \\ &+(2\chi_1^2-8\chi_3-8\chi_1\chi_3+2\kappa)\sigma_i^+\sigma_{i+3}^+|0\rangle \\ &+[4\chi_1^2+8\chi_1\chi_3-4\kappa(1+4\chi_1+\chi_3)-8\chi_1\chi_3^2]\sigma_i^+\sigma_{i+1}^+\sigma_{i+2}^+\sigma_{i+3}^+|0\rangle+\cdots\} \ . \end{aligned} \tag{39}$$

The requirement that the second, third, and fourth terms of Eq. (39) are zero leads to $\chi_1=0.3725$, $\chi_3=0.0372$, and $\kappa=0.0655$. The corresponding energy [first term of Eq. (39)] is then

$$E_0/NJ=-(1+2\chi_1)/2=-0.8725$$

(only 1.5% above the exact value—see Table I).

In comparison, the full SUB2 approximation, which allows all possible pair flips in S,

$$S=\sum_{i,n}\chi_n \sigma_i^+ \sigma_{i+n}^+ \ , \tag{40}$$

does not improve the energy substantially. Table II shows the results of a numerical solution of the equations

TABLE II. The fast decrease of nth neighbor spin-flip amplitudes χ_n within the SUB2 coupled-cluster approximation applied to the antiferromagnetic Heisenberg linear chain.

n	1	3	5	7	9	11	13
χ_n	0.337 244	0.021 654	0.002 884	0.000 487	0.000 093	0.000 019	0.000 004

with $n=15$ neighbors included in S. We observe a fast decrease of the χ_n's. The energy is $E_0/NJ=-0.8372$, only slightly better than the value obtained with the first elementary approximation. In conclusion, the succession of coupled-cluster approximations that we propose is more appropriate to the spin-lattice problem.

2. *The antiferromagnetic Heisenberg model on the square lattice*

We consider the Hamiltonian

$$H=\frac{J}{2}\sum_{i<j}^{(1)}\boldsymbol{\sigma}_i\cdot\boldsymbol{\sigma}_j \tag{41}$$

on a two-dimensional square lattice (the sum is restricted to nearest neighbors). In the Néel basis, the Hamiltonian (41) is transformed into an expression similar to Eq. (29). Using the diagrams of Fig. 1, the equations at the lowest level of the coupled-cluster approximation (CCA1) are obtained easily. The first-neighbor pair flip amplitude χ_1 is a solution of the equation

$$1-6\chi_1-5\chi_1^2=0 \quad \text{or} \quad \chi_1=0.148\,33 \tag{42a}$$

and the ground-state energy is

$$E_0/NJ=-(1+2\chi_1)=-1.2967\ . \tag{42b}$$

At the next level (CCA2), we include in S the terms that flip second neighbors (χ_2) and those that flip four spins on a square (κ_s). The system of coupled equations is

$$\begin{aligned}0&=-1+6\chi_1+5\chi_1^2-6\chi_2^2-2\kappa_s\ ,\\ 0&=\chi_1\chi_2+2\chi_2\ ,\\ 0&=-\chi_1^2+2\chi_1\chi_2^2+2\chi_1\kappa_s-\chi_2^2+\kappa_s\ ;\end{aligned} \tag{43}$$

The solution, $\chi_1=0.1531$, $\chi_2=0$, $\kappa_s=0.0179$, leads to a ground-state energy

$$E_0/NJ=-(1+2\chi_1)=-1.3062\ .$$

This energy is compared in Table I to molecular field, spin waves,[13] and a recent accurate variational calculation[16] using Monte Carlo methods. The accuracy (2%) is comparable to that obtained in one dimension. Although the energy correction with respect to the molecular field is smaller in two dimensions, we do not expect a better accuracy because the CCA2 cluster extends to a relatively shorter range.

B. The antiferromagnetic Heisenberg linear chain in a magnetic field

We now illustrate the coupled cluster method in a slightly more complicated situation where the spin directions in the Néel state are not aligned. In a magnetic field, the Zeeman term

$$H_Z=-B\sum_i\sigma_i^z \tag{44}$$

is added to the Hamiltonian (28). The molecular-field state has two sublattices with spin directions at angles θ and $-\theta$ from the magnetic field. The angle θ is given by

$$\cos(\theta)=B/B_c\ , \tag{45}$$

where $B_c=2J$ represents the transition field to the ferromagnetic state, and the magnetization increases linearly with B up to B_c. The Hamiltonian is easily transformed into the Néel basis

$$\begin{aligned}H=\frac{J}{2}\sum_{i=1}^{N}\{&[\cos(2\theta)-1](\sigma_i^-\sigma_{i+1}^-+\sigma_i^+\sigma_{i+1}^+)+[\cos(2\theta)+1](\sigma_i^-\sigma_{i+1}^++\sigma_i^+\sigma_{i+1}^-)\\&+(-1)^i\sin(2\theta)[\sigma_i^z(\sigma_{i+1}^-+\sigma_{i+1}^+)-\sigma_{i+1}^z(\sigma_i^-+\sigma_i^+)]+\cos(2\theta)\sigma_i^z\sigma_{i+1}^z\}\\&+B\sum_{i=1}^{N}[\cos(\theta)\sigma_i^z-(-1)^i\sin(\theta)(\sigma_i^-+\sigma_i^+)]\ .\end{aligned} \tag{46}$$

The spin axes have been chosen to avoid imaginary terms in this expression: The y axis is fixed and (x,z) are rotated around y.

In contrast to the simple examples studied in Sec. III A there are some terms in the Hamiltonian that at the most elementary CCA1 level generate new linear $\sigma_i^+|0\rangle$ terms in $\bar{H}|0\rangle$, which are proportional to χ_{ij}. In order to satisfy the relation (21) with $\langle n|$ corresponding to one-spin-flipped states, we have to reintroduce in S the operators that flip one spin, $\alpha_i\sigma_i^+$, to balance these new terms. At the next CCA2 level, together with the pair- and four-spin flips, we also have to take into account in S the terms that flip three spins: $\tau_i\sigma_i^+\sigma_{i+1}^+\sigma_{i+2}$,

$$\begin{aligned}S=\sum_{i=1}^{N}(&\alpha_i\sigma_i^++\chi_1\sigma_i^+\sigma_{i+1}^++\chi_2\sigma_i^+\sigma_{i+2}^++\chi_3\sigma_i^+\sigma_{i+3}^+\\&+\tau_i\sigma_i^+\sigma_{i+1}^+\sigma_{i+2}^++\kappa\sigma_i^+\sigma_{i+1}^+\sigma_{i+2}^+\sigma_{i+3}^+)\ .\end{aligned} \tag{47}$$

As already emphasized, the action of $\exp(\alpha_i^+\sigma_i^+)$ on $|0\rangle$,

$$\exp(\alpha_i^+\sigma_i^+)|0\rangle=(1+\alpha_i^+\sigma_i^+)|0\rangle\ , \tag{48}$$

induces a rotation of angle $\theta_i=\arctan(\alpha_i)$ for the spin i. In order to preserve the symmetry of the two sublattices with respect to the direction of the magnetic field we have to take opposite value of the α_i's

$$\alpha_i=(-1)^i\alpha \quad \text{and} \quad \tau_i=(-1)^i\tau \ . \tag{49}$$

Starting from the molecular field state $|0\rangle$, the parameters α,χ_n $(n=1,2,3),\tau,\kappa$ in S [cf. Eq. (47)] can be determined from the set of coupled equations (21), $|n\rangle$ representing excited states with one, two, three, and four spin flips.

There is a simpler alternative that we would rather use. We may as well readjust the angle θ, slightly away from molecular-field value in order that the preceding set of equations has $\alpha=0$ as a solution. The calculations are simpler, and we thus start from a $|0\rangle$ state that in principle should be closer to the exact ground state than the Néel state.

The ground-state energy's dependence on the magnetic field B is represented in Fig. 2. The CCA1 (short-dashed line) and CCA2 (long-dashed line) coupled-cluster approximations are compared to the molecular field (dotted line) and to the exact result of Griffiths[17] (solid line).

The CCA2 curve is sufficiently close to the exact result for a reasonable estimate of the magnetization to be obtained by simply differentiating

$$M=-\partial E(B)/\partial B \ . \tag{50}$$

The results are shown in Fig. 3 (dashed line) and compared to the molecular field (dotted line) and Griffiths exact result[17] (solid line). Except in the neighborhood of the critical field where the exact result exhibits an infinite slope, the agreement is good. The inset shows the variations of the angle θ [we have plotted $\cos(\theta)$ in terms of B/B_c], which, for each value of the field, is readjusted as explained before (dashed line). There is a large departure from mean field (dotted line), which corresponds to the fact that the exact zero field susceptibility is much lower than the molecular field estimate.

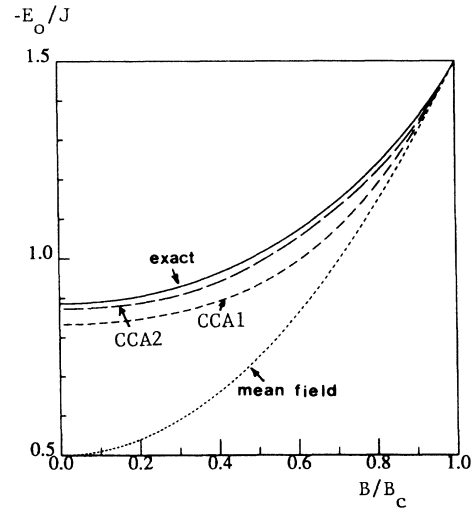

FIG. 2. Energy of the antiferromagnetic Heisenberg linear chain as a function of the magnetic field ratio B/B_c. $B_c=2J$ is the transition field to the ferromagnetic phase. The coupled cluster approximation for two cluster sizes: CCA1 (short-dashed line), CCA2 (long-dashed line) is compared to mean-field (dotted line) and the exact result of Griffiths[17] (solid curve).

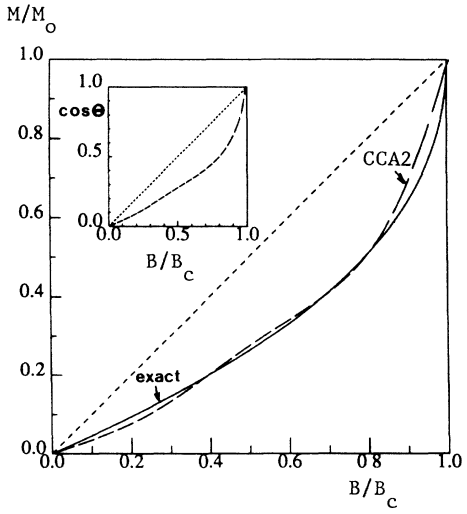

FIG. 3. Reduced magnetization M/M_0, as a function of the magnetic field ratio B/B_c for the antiferromagnetic Heisenberg linear chain. $B_c=2J$ is the transition field to the ferromagnetic phase. The coupled-cluster approximation CCA2 (dashed line) is compared to molecular field (dotted line) and exact result of Griffiths[17] (solid curve). The inset shows $\cos(\theta)$, for the coupled cluster (dashed line) and for the mean field (dotted line) as a function of the same ratio. θ is the angle between sublattice spin direction and the applied field.

C. The frustrated linear chain

Here we study the Heisenberg linear chain with competing antiferromagnetic interactions between first and second neighbors. The Hamiltonian is

$$H=\frac{J}{2}\sum_{i=1}^{N}(\boldsymbol{\sigma}_i\cdot\boldsymbol{\sigma}_{i+1}+\eta\boldsymbol{\sigma}_i\cdot\boldsymbol{\sigma}_{i+2}) \ . \tag{51}$$

It is suitably represented by a railroad-trestle lattice (Fig. 4), which for $\eta=\frac{1}{2}$ may be viewed as a piece of the frustrated triangular lattice. It has been shown that for $\eta=\frac{1}{2}$, the RBV wave function [Eq. (36)], is an exact ground state[18] with energy $E_0/J=-0.75$. We shall study it for $0<\eta<\frac{1}{2}$.

The molecular-field state is a simple alternate antiferromagnetic phase (cf. Sec. III A) up to $\eta=0.25$. Then the stable phase is helimagnetic. For simplicity, we shall keep the simple antiferromagnetic phase over the whole range $0<\eta<\frac{1}{2}$ as a $|0\rangle$ state (if we start from a helical phase, the form to give to the three-spin-flip amplitudes τ_{ijk} is not straightforward). As we shall see, the results obtained in this way are satisfying for the range $0<\eta<\frac{1}{2}$ that we study.

At the first CCA1 level, we include in S the terms that flip pairs of first neighbors (χ_1) and second neighbors (χ_2). With the help of Fig. 1, the following equations are easily obtained:

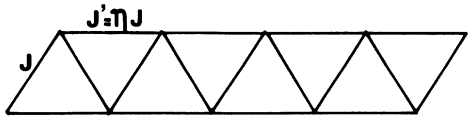

FIG. 4. The railroad-trestle lattice.

$$0=-2+4(1-\eta)\chi_1+6\chi_1^2-4\chi_2^2 ,$$
$$0=(8-4\eta)\chi_2+8\chi_1\chi_2 . \tag{52}$$

The physical solution is

$$\chi_2=0 \text{ and } \chi_1=\frac{\eta-1+[(1-\eta)^2+3]^{1/2}}{3} . \tag{53}$$

The energy

$$E_0/NJ=-(1-\eta+2\chi_1)/2$$

is represented in Fig. 5 (short-dashed line).

The next order (CCA2) is solved by computer. We include pair flips up to third neighbors and four-spin flips (κ). The results are compared in Fig. 5 (long-dashed line) with an accurate estimate based on extrapolation to infinite lattice of exact calculations on finite chains[19] (solid curve). The accuracy is better than 2% on the whole range (although for $\eta\approx 0.4$–0.5 the exact energy is about twice the molecular-field value). However, we certainly would have to go to much higher orders to reproduce the maximum of the exact curve at $\eta=0.5$. This feature is related to a peculiarity of the exact RVB ground state, which has zero correlations between second neighbors, hence

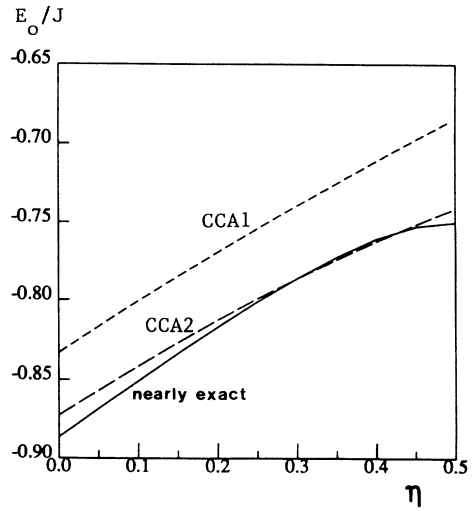

FIG. 5. The ground-state energy of the frustrated antiferromagnetic Heisenberg linear chain as a function of the ratio η of second to first neighbor interactions. The CCA1 (short-dashed line) and CCA2 (long-dashed line) coupled-cluster approximations are compared to nearly exact results[19] (solid curve).

$$\frac{\partial E}{\partial \eta}=\text{const}\times\langle\boldsymbol{\sigma}_i\cdot\boldsymbol{\sigma}_{i+2}\rangle=0 .$$

As noted in Sec. III A, the RVB wave function is included in our formalism if we allow unequal χ between left and right neighbors. Including this possibility we obtain the RVB state as a solution for $\eta=0.5$. However, at the CCA1 level, if we follow that solution slightly away from $\eta=0.5$, we do not reproduce the maximum either and E moves rapidly away from the exact solution. Further studies are needed around that point; they are beyond the scope of this paper.

IV. THE SPIN SYSTEM IN ^{3}He

A. The multiple-exchange Hamiltonian

The general spin-exchange Hamiltonian is written[2–6]

$$H_{\text{ex}}=-\sum_{P^\sigma}(-1)^p J_P P^\sigma , \tag{54}$$

where the sum runs over all permutations P^σ acting on N spin variables. $(-1)^p$ represents the sign of the permutation P. A general result, first shown by Thouless,[20] is that even and odd permutations respectively favor ferromagnetism and antiferromagnetism, and all J_P's in Eq. (54) have the same positive sign. If the only relevant permutations are pair transpositions, $P_{ij}=(1+\boldsymbol{\sigma}_i\cdot\boldsymbol{\sigma}_j)/2$, where $\boldsymbol{\sigma}_i$ represent Pauli spin operators, we obtain the usual Heisenberg Hamiltonian.

Due to the hard-core interactions between exchanging fermions, two, three, and four particle cyclic exchange processes are of the same order of magnitude in solid ^{3}He.[2–6] Although they are smaller, six-particle exchange processes might play a significant role in the high-field phase of bcc ^{3}He.[6,8]

Three particle permutations $P_{ijk}=P_{ij}P_{ik}$ reduce to effective Heisenberg interactions:

$$P_{ijk}+P_{ijk}^{-1}=(1+\boldsymbol{\sigma}_i\cdot\boldsymbol{\sigma}_j+\boldsymbol{\sigma}_j\cdot\boldsymbol{\sigma}_k+\boldsymbol{\sigma}_k\cdot\boldsymbol{\sigma}_i)/2 . \tag{55}$$

Cyclic four-spin permutations $P_{ijkl}=P_{ij}P_{ik}P_{il}$ give new fourth-order terms:[3,20]

$$P_{ijkl}+P_{ijkl}^{-1}=\frac{1}{4}\left[\sum_{\alpha<\beta}\boldsymbol{\sigma}_\alpha\cdot\boldsymbol{\sigma}_\beta+\mathcal{G}_{ijkl}\right] \tag{56}$$

the sum $\sum_{\alpha<\beta}$ is performed over all distinct pairs in $\{i,j,k,l\}$ and

$$\mathcal{G}_{ijkl}=(\boldsymbol{\sigma}_i\cdot\boldsymbol{\sigma}_j)(\boldsymbol{\sigma}_k\cdot\boldsymbol{\sigma}_l)+(\boldsymbol{\sigma}_j\cdot\boldsymbol{\sigma}_k)(\boldsymbol{\sigma}_l\cdot\boldsymbol{\sigma}_i)-(\boldsymbol{\sigma}_i\cdot\boldsymbol{\sigma}_k)(\boldsymbol{\sigma}_j\cdot\boldsymbol{\sigma}_l) . \tag{57}$$

In the Néel basis, each dot product $\boldsymbol{\sigma}_i\cdot\boldsymbol{\sigma}_j$ is transformed into the general expression

$$\cos(\theta_i-\theta_j)(\sigma_i^x\sigma_j^x+\sigma_i^z\sigma_j^z)+\sin(\theta_i-\theta_j)(\sigma_i^z\sigma_j^x-\sigma_i^x\sigma_j^z)+\sigma_i^y\sigma_j^y , \tag{58}$$

where θ_i represents the angle of the local mean field at site i, with respect to some arbitrary origin. Here again the y axis is fixed and (x,z) are rotated around y from one site to the other. In that way the expression of the Ham-

iltonian in the mean-field basis is real. Substituting Eq. (58) into the relations (55)–(57) the Hamiltonian is transformed into the general form (3), or into (8) if we use the Eqs. (4).

B. Four-spin exchange in the 2D square lattice

Two-dimensional Heisenberg ferromagnetism has recently been observed in two ^{3}He solid layers adsorbed on grafoil.[21] On that substrate, the ^{3}He lattice is triangular and three-particle exchange processes are expected to be preponderant.[2,5] A coherent interpretation of the experimental results[21] has been proposed within the multiple-exchange model.[22]

In principle, using some appropriate substrate presenting a sufficiently strong adsorption potential with a quadratic symmetry, a commensurate square lattice of ^{3}He atoms could be stabilized (a MgO powder substrate might be a good candidate[23]). In a square lattice, four-particle exchange processes should dominate,[2,5] leading, in contrast, to antiferromagnetism. As we shall see, the experimental results should even be more exciting in that case. Four-spin exchange might also be relevant in the two-dimensional CuO_2 planes of copper based new superconducting ceramics.[24]

Besides this important experimental interest, the four-spin exchange Hamiltonian in two dimensions already presents the essential features observed in three dimensional bcc ^{3}He, with the theoretical advantage that the coupled-cluster approximation can be compared to exact calculations on finite clusters with reasonable size.

In a two-dimensional square lattice, we expect pair exchange between first neighbors (J_{NN}) and four-spin exchange on a square (K_s) to be the most important exchange processes (see Fig. 6). Using Eqs. (55)–(57), the Hamiltonian (54) is written

$$H_{ex}=\frac{J_1}{2}\sum_{i<j}^{(1)}\sigma_i\cdot\sigma_j+\frac{J_2}{2}\sum_{i<j}^{(2)}\sigma_i\cdot\sigma_j + \frac{K_s}{4}\sum_{i<j<k<l}^{(sq)}\left[\sum_{\alpha<\beta}\sigma_\alpha\cdot\sigma_\beta+\mathcal{G}_{ijkl}\right]+E_P \ . \tag{59}$$

J_1 and J_2 are effective pair exchange interactions between first and second neighbors

$$\begin{aligned} J_1&=J_{NN}+K_s \ , \\ J_2&=K_s/2 \ . \end{aligned} \tag{60}$$

The constant

$$E_P=N(J_{NN}+K_s/4)$$

represents the energy of the Hamiltonian (54) in the paramagnetic phase at infinite temperature. In all that follows, E_P will be chosen as the origin for energies.

For $\eta=J_{NN}/K_s>0.5$, the zero-field Néel state is a normal two-sublattice antiferromagnetic ("NAF") phase [Fig. 6(a)]. For $\eta<0.5$ the molecular-field state is a four-sublattice phase with orthogonal magnetizations shown in Fig. 6(c). The energies of the two phases are, respectively,

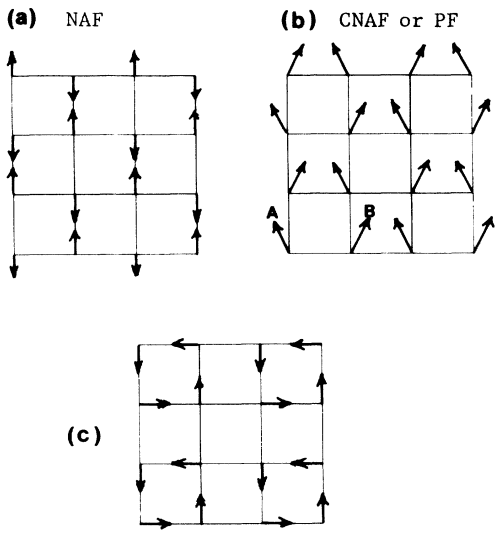

FIG. 6. The normal antiferromagnetic NAF phase (a) the CNAF or PF phase (b) and the four-sublattice phase with orthogonal magnetizations (c) on a two-dimensional square lattice.

$$\begin{aligned} E_{NAF}/N&=-J_{NN}-K_s/4 \ , \\ E_\perp/N&=-3K_s/4 \ . \end{aligned} \tag{61}$$

For all values of η, the high-field molecular-field state is a canted normal antiferromagnetic phase (CNAF)—see Fig. 6(b). This phase has two sublattices A and B with respective magnetizations at angles θ and $-\theta$, symmetric with respect to the magnetic field with

$$4J_{NN}\cos(\theta)+8K_s\cos^3(\theta)=B \ . \tag{62}$$

With four-spin exchange, the second term in (62) leads to a strong enhancement of the magnetization $M=M_0\cos(\theta)$ (M_0 representing the saturation value). This phase is identical to the so-called "pseudoferromagnetic (PF)" phase observed in bcc ^{3}He.[3] Its energy is

$$E_{PF}/N=2J_{NN}\cos^2(\theta)+2K\cos^4(\theta) -B\cos(\theta)-K_s/4-J_{NN} \ , \tag{63}$$

θ being given by (62). It undergoes a second-order transition to the ferromagnetic phase at a critical field

$$B_{c2}=4(J_{NN}+2K_s) \ . \tag{64}$$

(Note that the molecular-field value of this transition field is indeed exact.[3,8]) For $\eta<0.5$, there is, at a relatively low-field—compared to B_{c2}—a first-order transition from the four-sublattice phase to the "PF" phase.

In order to test the accuracy of the coupled-cluster approximation on this Hamiltonian, we have first estimated the ground-state energy by the general methods used in the literature for low-dimensional Heisenberg or XY models.[25,26] Exact ground-state energies are calculated with the Lanczös[27] method for finite systems of $N=4$–20 particles. Extrapolation of energy plots as a function of $1/N$ are made to estimate the ground-state energy for the

infinite system.

We first apply the method of Ref. 25. The exact ground-state energy is calculated for the finite clusters of $N=4,8,16,18$ particles, represented in Fig. 7, with periodic boundary conditions (the $N=10$ or 24 particle clusters used for the Heisenberg model[25] are not suitable here, due to their peculiar unsymmetrical boundary conditions, see Fig. 7). The energies are plotted in Fig. 8 as a function of $1/N$ for a pure four-spin exchange Hamiltonian ($J_{NN}=0$). A least-squares quadratic fit (solid line) extrapolates to

$$E_0/NK_s=-1.14 \tag{65}$$

for the infinite lattice, a value much smaller than the mean-field estimate $E_{MF}/NK_s=-0.75$.

We can also adapt to our problem another method used more recently[26] for the triangular lattice. The exact ground-state energies are calculated for successive rows of four-spin cycles with length l and width w (see Fig. 9) with free boundaries. For each fixed width w, the energy is plotted as a function of $1/l$ and a value $E(l=\infty,w)$ is deduced for infinite length through a straight line extrapolation (cf. Fig. 9). In inset the values of $E(l=\infty,w)$ such obtained are plotted as a function of $1/w$. An estimate of the ground-state energy

$$E_0/NK_s=-1.18\pm0.05 \tag{66}$$

is deduced for the infinite system from a straight line extrapolation.

We now apply the coupled-cluster approximation to the four-spin exchange Hamiltonian. The lowest order should include all pair- and four-spin flips in S which are already generated by the Hamiltonian:

$$S=\chi_1\sum_{i<j}^{(1)}\sigma_i^+\sigma_j^+ +\chi_2\sum_{i<j}^{(2)}\sigma_i^+\sigma_j^+ +\kappa_s\sum_{i<j<k<l}^{(sq)}\sigma_i^+\sigma_j^+\sigma_k^+\sigma_l^+ \ . \tag{67}$$

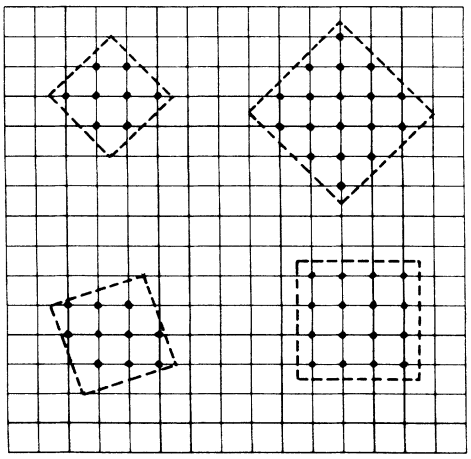

FIG. 7. Finite square clusters of various size with periodic boundary conditions in the two-dimensional square lattice.

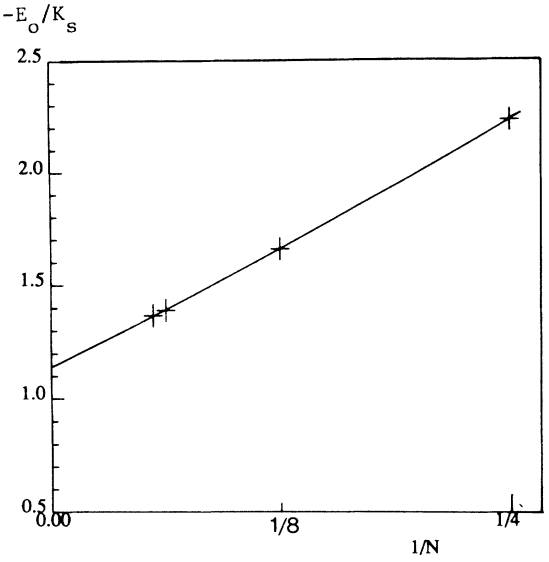

FIG. 8. Exact ground-state energies for N particle square clusters with periodic boundary conditions as a function of $1/N$.

The two first sums are restricted to first and second neighbors, respectively, and the third is performed over distinct square four-spin cycles. Starting from the mean-field four-sublattice state [Fig. 6(c)], we obtain for $J_{NN}=0$ a ground-state energy $E_0/NK_s=-1.16$, in good agreement with the previous estimates [Eqs. (65) and

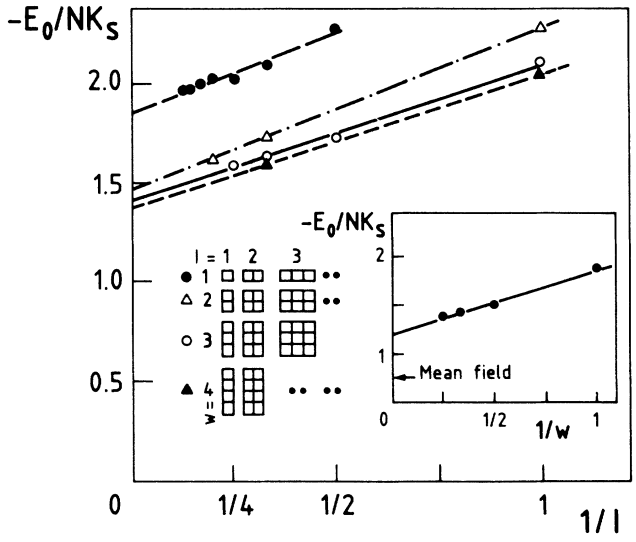

FIG. 9. Exact ground-state energies for successive rows of four-particle cycles with length l and width w. For fixed width, the energies are plotted as a function of $1/l$ and linearly extrapolated to $l\to\infty$. Each of the extrapolated values is plotted in the inset as a function of $1/w$. An estimate of the energy $E_0/(NK_S)=-1.18\pm0.05$ for the infinite system $l\to\infty, w\to\infty$ is deduced.

(66)]. The values of the three parameters in S are $\chi_1=0.1566$, $\chi_2=0.0434$, and $\kappa_s=0.0605$.

It is worth noticing that the study of spin correlations on the exact ground state of finite systems, with the same $1/N$ extrapolation methods,[25,26] proves that the staggered magnetization of the four-sublattice phase tends to zero for the infinite system (see Ref. 24 for more details). In contrast, a two sublattice long-range order seems to subsist for $N\rightarrow\infty$ with large fluctuations (cf. Fig. 2 of Ref. 24). However, if we start from the two-sublattice "NAF" phase as $|0\rangle$ state for the coupled-cluster approximation, we obtain $E_0/NK_s=-0.9166\ldots$ with $\chi_1=\chi_2=0$ and $\kappa_s=-0.3333\ldots$. This energy value is much lower than the mean-field value $E_{\rm NAF}/NK_s=-0.25$ [cf. relation (61)] but still higher than our best estimate $E_0/NK_s=-1.18\pm0.05$ [see Eqs. (65)–(66)].

It is also interesting to check the accuracy of the coupled-cluster approximation in the presence of both first-neighbor pair exchange and four-spin exchange. With $J_{\rm NN}=K_s$, starting from the NAF phase, which is the stable state in mean field, the coupled-cluster approximation gives $E_0/NK_s=-1.70$ with $\chi_1=0.06$, $\chi_2=0$, and $\kappa_s=-0.17$. The energy is close to the estimate based on extrapolations of exact results on $N=4,8,16,18$ particle clusters using the method described in Fig. 7: $E_0/NK_s=-1.76$. (Starting from the four-sublattice phase as $|0\rangle$, we obtain a higher value $E_0/NK_s=-1.46$.)

As already noted, the "CNAF" phase with enhanced magnetization, or "PF" phase, is always stable at high field for any value of the parameter ratio $\eta=J_{\rm NN}/K_s$. We now apply the coupled-cluster approximation in arbitrary magnetic field starting from the PF state. With pair- and four-spin flips [Eq. (67)], we have to include in S the terms that flip three spins on a triangle with two first-neighbor and one second-neighbor pairs:

$$S=\chi_1\sum_{i<j}^{(1)}\sigma_i^+\sigma_j^+ +\chi_2\sum_{i<j}^{(2)}\sigma_i^+\sigma_j^+ +\sum_{i<j<k}^{(T)}\tau_{ijk}\sigma_i^+\sigma_j^+\sigma_k^+ +\kappa_s\sum_{i<j<k<l}^{(sq)}\sigma_i^+\sigma_j^+\sigma_k^+\sigma_l^+ \ . \tag{68}$$

As explained in Sec. III B, to conserve the symmetry of the two alternate sublattices with respect to the magnetic field, τ_{ijk} must change sign for all symmetries which exchange the two sublattices A and B:

$$\tau_{ijk}=\tau$$

for a triangle with two A and one B spins ,

$$\tau_{ijk}=-\tau \tag{69}$$

for a triangle with two B and one A spins.

The procedure is the same as discussed in Sec. III B. The angle θ is readjusted with respect to the mean-field value and $\chi_1,\chi_2,\tau,\kappa_s$ are determined in order to satisfy the coupled system of Eqs. (21).

The quantity that is the most interesting and accessible to experiments is the magnetization. We have proved in Sec. III B that a good estimate can be obtained by differentiation of the energy with respect to B [relation (50)].

Figures 10(a)–10(f) shows the evolution of the magnetization curve as a function of the parameter ratio $\eta=J_{\rm NN}/K_s$. The results of the coupled-cluster approximation (dashed lines) are compared to mean field (dotted lines) and exact results (solid staircases) for a finite 16-particle system with periodic boundary conditions. The most exciting result is a "plateau," which is observed in a range $0.1<B/B_{c2}<0.4$ with a slowly varying but relatively high magnetization $M\approx0.5M_0$. This striking behavior, which does not appear within molecular-field approximation, is exhibited by both the coupled-cluster approximation and exact results on finite systems. It should be the most interesting feature to observe experimentally

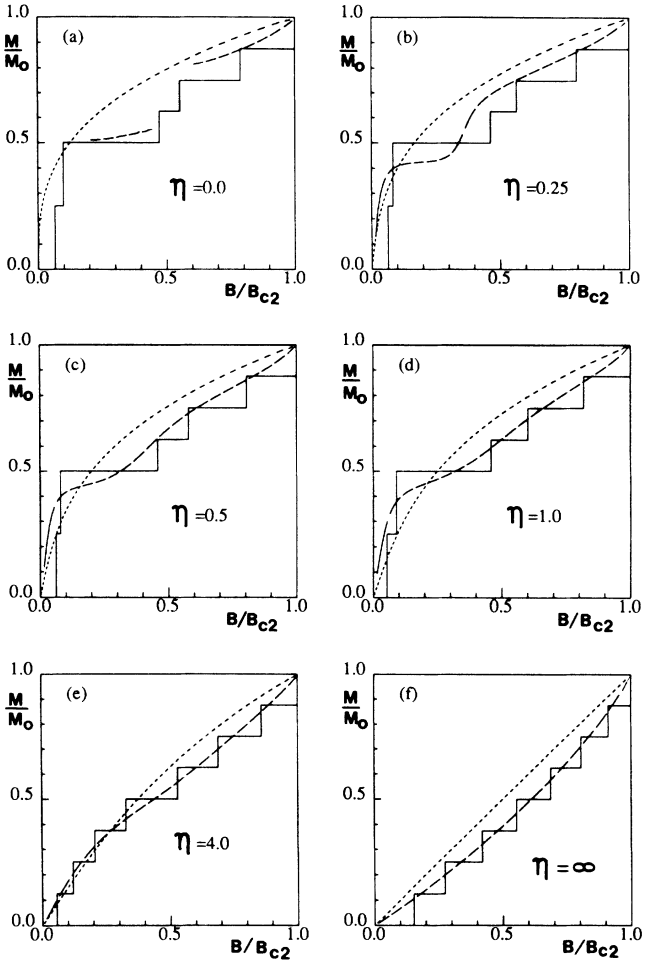

FIG. 10. The reduced magnetization M/M_0 for the PF phase of the two-dimensional square lattice with pair ($J_{\rm NN}$) and four-particle exchange (K_s) as a function of B/B_{c2}. Figures (a) to (f) are for various values of the parameter ratio $\eta=J_{\rm NN}/K_s$. B_{c2} is the transition field to the ferromagnetic state. The coupled cluster approximation (dashed lines) is compared to the molecular field (dotted lines) and to exact results for a 4×4 particle cluster with periodic boundary conditions (solid staircases).

(e.g., for ^{3}He adsorbed on an appropriate substrate with a commensurate square lattice). As η increases this plateau is smeared out; however, a strong enhancement of the magnetization subsists at low field, even for relatively low values of K_s [see Fig. 10(e) with $K_s = J_{NN}/4$]. The enhancement of the magnetization at low field is a characteristic property of four-spin exchange interactions. It is also seen at finite temperature in the zero-field susceptibility, which has been theoretically calculated through high-temperature series expansions[28] and exact results on finite systems.[24] The corresponding variations of the angle θ (dashed lines) and energies (solid lines) are shown in Fig. 11. The angle θ differs appreciably from the mean-field value (dotted lines) and already accounts for the shape of the magnetization curve (Fig. 10) with a flat region for $0.1 < B/B_{c2} < 0.4$.

The first figures of each set [10(a) and 11(a)], corresponding to a pure four-spin Hamiltonian ($J_{NN}=0$), show evidence of a technical difficulty. The set of coupled-cluster equations (21) does not have a real solution in the range $0.15 < B/B_{c2} < 0.5$. Two procedures are then possible: (i) We can take the complex solution and retain the real part of the energy or (ii) we can keep the parameters in S real and optimize them by minimizing the sum of the squares of the second members of Eqs. (21). We chose the second alternative, but the results of the two methods are not significantly different on the scale of Figs. 10(a) and 11(a). The singularities in the magnetization which are evident in those figures result from the change in methodology at the end points of this region.

The last figures [10(f) and 11(f) of each set] correspond to the pure Heisenberg model on the two-dimensional square lattice. Another important feature to be noticed is that, in contrast to the molecular-field result, the second derivative of the magnetization curve is negative just below the transition field B_{c2} for all values of the parameter ratio η.

In conclusion, we have found by comparison to exact calculations on finite clusters of $N=4$–20 particles that the coupled cluster approximation also works quite well for fourth-order interactions such as are found in the multiple-exchange Hamiltonian. Some interesting predictions on the shape of the magnetization curve have been made with four-spin exchange on a two-dimensional square lattice.

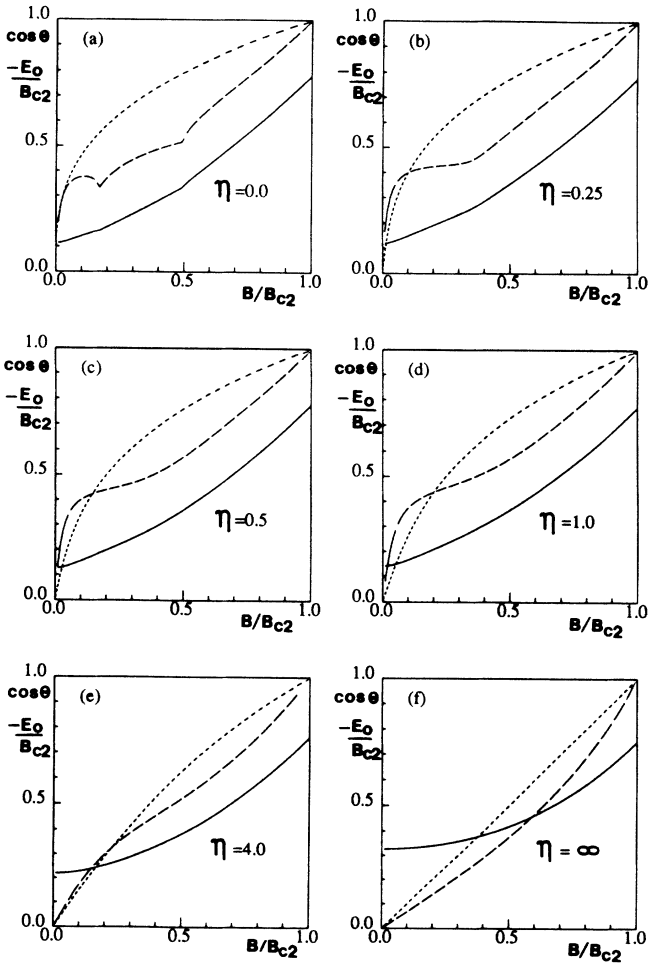

FIG. 11. The ground-state energies (solid curves), $\cos(\theta)$ (dashed lines), within CCA and molecular-field values of $\cos(\theta)$ (dotted lines) as a function of B/B_{c2} for the same parameter values as in Fig. 10. θ is the angle between the sublattice magnetization and the applied magnetic field.

C. The bcc phase of solid ^{3}He

1. Generalities

One peculiarity of bcc ^{3}He magnetism is that some parameters, such as the first coefficients of the high-temperature series expansions of thermodynamic data, which can be calculated exactly, are difficult to measure accurately. In contrast, some quantities, as the first-order transition field between the two ordered phases, which have long been measured with precision, are the most difficult to predict theoretically. Our first motivation in this work was to obtain a reasonable estimate of this transition field.

Two ordered phases have been observed experimentally in the millikelvin range.[3,4] In zero field there is a four-sublattice antiferromagnetic state: the so-called "UUDD" phase [Fig. 12(a)]. All spins have the same orientation in a given (100) plane and, along the direction (100) the spins alternate in a sequence of two "up" planes, two "down" planes. . . . This structure was first suggested by nuclear magnetic resonance experiments and later confirmed by neutron diffraction.[29] At a relatively low field ($B_{c1}=0.45$ T at $T\to 0$), there is a first-order transition to another magnetic state with cubic symmetry [Fig. 12(b)], which presents all features of the PF phase described in the previous subsection. The magnetization of this phase is already of order $0.5M_0$ at the (relatively small) transition field B_{c1}. The second-order transition field B_{c2} to the ferromagnetic state is thought to be of order 20 T, on the basis of recent experimental investigations.[30] Hence with a ratio $B_{c1}/B_{c2} \approx 0.02$ we see that these two phases, degenerate at B_{c1}, are almost degen-

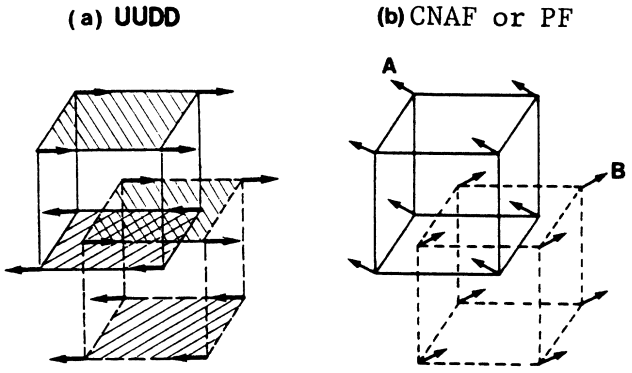

FIG. 12. The UUDD and CNAF or PF phases in the bcc lattice of solid ^{3}He.

erate at zero field. This is the major difficulty in predicting B_{c1} theoretically.

Although the main qualitative features of the phase diagram are provided by the preponderant exchange processes[3,4] (pair exchange between first neighbors, J_{NN}; triple exchange on the most compact triangles, J_T; and cyclic four-spin exchange on planar cycles with four first neighbors, K_P, see Fig. 13), calculations from first principles[5,6] have revealed that the exchange frequencies do not decrease with the number of particles involved as fast as previously conjectured. Some higher processes (six-spin ring exchanges, etc.), although smaller, should be taken into account in quantitative theoretical predictions. We shall first apply the coupled-cluster approximation to a model including the three dominating exchange processes: J_{NN}, J_T, and K_P. "Mean-field corrections" (in a sense that will appear in the following) will be added to take into account smaller exchanges as six-spin cyclic permutations. A fully consistent treatment of six-spin interactions within coupled-cluster approximation is possible in the future. It represents a large amount of work but will be worthwhile if more accurate Monte Carlo calculations of these small exchange frequencies are available.

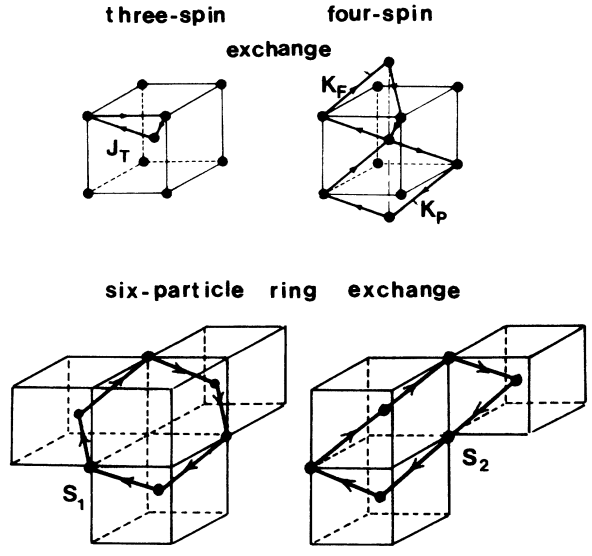

FIG. 13. The main ring-exchange cycles in bcc ^{3}He.

2. *Retaining only the main exchange processes*

We consider the following multiple exchange Hamiltonian:

$$H_{ex}=J_{NN}\sum_{i<j}^{(1)}P_{ij}+J_{NNN}\sum_{i<j}^{(2)}P_{ij}-J_T\sum_{i<j<k}^{(T)}(P_{ijk}+P_{ijk}^{-1})+K_P\sum_{i<j<k<l}^{(Pl)}(P_{ijkl}+P_{ijkl}^{-1}), \tag{70}$$

where P_{ij}, P_{ijk}, and P_{ijkl} represent cyclic permutations of two, three, and four spins, respectively. The sums are performed on first (1) and second (2) neighbor pairs, the most compact triangles (T) and planar four-spin cycles (Pl) (see Fig. 13). (Although small, we have also included second-neighbor pair exchange because it does not complicate the treatment of the Hamiltonian). When the permutation operators are expressed in terms of Pauli-spin matrices [cf. Eqs. (55)–(57)], we obtain

$$H_{ex}=\frac{J_1}{2}\sum_{i<j}^{(1)}\boldsymbol{\sigma}_i\cdot\boldsymbol{\sigma}_j+\frac{J_2}{2}\sum_{i<j}^{(2)}\boldsymbol{\sigma}_i\cdot\boldsymbol{\sigma}_j+\frac{J_3}{2}\sum_{i<j}^{(3)}\boldsymbol{\sigma}_i\cdot\boldsymbol{\sigma}_j+\frac{K_P}{4}\sum_{i<j<k<l}^{(Pl)}\left[\sum_{\alpha<\beta}\boldsymbol{\sigma}_\alpha\cdot\boldsymbol{\sigma}_\beta+\mathcal{G}_{ijkl}\right]+E_P \tag{71}$$

J_1, J_2, and J_3 are effective pair exchange interactions between first, second, and third neighbors

$$\begin{cases}J_1=J_{NN}+3(-2J_T+K_P)\\J_2=J_{NNN}-4J_T+K_P\\J_3=K_P/2\end{cases} \tag{72}$$

$\mathcal{G}_{ijkl}$ is given by (57) and

$$E_P=N(2J_{NN}+3J_{NNN}/2-6J_T+3K_P/2)$$

is a constant which will be taken as the origin for energies in all that follows.

At the lowest level of the coupled-cluster approximation one should include in S all n-spin flips generated by the Hamiltonian itself: pair flips between first, second, and third neighbors, three-spin flips on the most compact triangles, four-spin flips on planar four-site cycles.

(i) The PF phase.

We take

$$S_{PF}=\chi_1\sum_{i<j}^{(1)}\sigma_i^+\sigma_j^++\chi_2\sum_{i<j}^{(2)}\sigma_i^+\sigma_j^++\chi_3\sum_{i<j}^{(3)}\sigma_i^+\sigma_j^++\sum_{i<j<k}^{(T)}\tau_{ijk}\sigma_i^+\sigma_j^+\sigma_k^++\kappa_P\sum_{i<j<k<l}^{(Pl)}\sigma_i^+\sigma_j^+\sigma_k^+\sigma_l^+ . \tag{73}$$

As explained in Sec. IV A, to conserve the symmetry of the two alternate sublattices with respect to the magnetic field, τ_{ijk} is chosen according to the rule (69).

$$\tau_{ijk}=\tau$$

for a triangle with two A and one B spins.

$$\tau_{ijk}=-\tau$$

for a triangle with two B and one A spins.

The procedure is the same as defined in Secs. III B, IV A: in arbitrary magnetic field B, the angle θ is readjusted with respect to the mean-field value and χ_1, χ_2, χ_3, τ, and κ_P are determined in order to satisfy the coupled system of Eqs. (21).

(ii) The UUDD phase.

In this case, we shall restrict the coupled-cluster calculation to the zero-field case. The experimental transition field B_{c1} to the "PF" state is so small ($B_{c1}/B_{c2}\approx 0.02$) that its energy is always very close to the zero-field value. (A correction $-\chi_{\mathrm{MF}}B^2/2$, where χ_{MF} represents the molecular-field susceptibility will be taken into account in the calculation of the transition field B_{c1}).

This phase needs more parameters since, with four tetragonal magnetic sublattices [Fig. 12(a)], its symmetry is lower. Each of the first, second, and third neighbor pair flips are partitioned into two subgroups: (χ_1^a,χ_1^b), (χ_2^a,χ_2^b), (χ_3^a,χ_3^b) depending whether they correspond to antiferromagnetic or ferromagnetic bonds, respectively. All planar four-spin cycles have three spins in the same direction and the fourth one in opposite direction, however, they can be classified into two kinds (κ_P^a,κ_P^b), depending whether the spins on second-neighbor links are identical or not (see Fig. 14). There are no three-spin flips in zero field.

$$S_{\mathrm{UUDD}}=\sum_{\lambda=a,b}\left[\chi_1^\lambda\sum_{i<j}^{(1^\lambda)}\sigma_i^+\sigma_j^+ +\chi_2^\lambda\sum_{i<j}^{(2^\lambda)}\sigma_i^+\sigma_j^+ +\chi_3^\lambda\sum_{i<j}^{(3^\lambda)}\sigma_i^+\sigma_j^+ +\kappa_P^\lambda\sum_{i<j<k<l}^{(Pl^\lambda)}\sigma_i^+\sigma_j^+\sigma_k^+\sigma_l^+\right] . \quad (74)$$

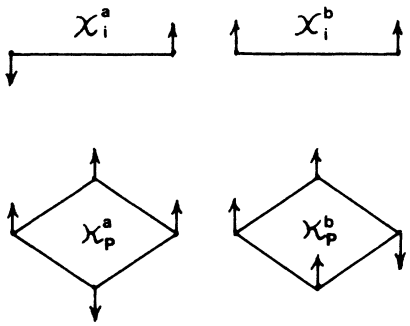

FIG. 14. Different spin configurations for various cycles of the UUDD phase in bcc ^{3}He.

The index λ refers to the partition shown in Fig. 14.

We choose the parameters determined by Monte Carlo calculations[6] (cf. Table III) adjusted from $v=24.12$ cm^3/mol to the melting molar volume 24.22 cm^3/mol with a scaling factor v[18] [the "Grüneisen" coefficients $\Gamma=\partial\ln(J_P)/\partial v$ are of the same order, $16<\Gamma<20$, for all important exchange parameters[5,6]]:

$$J_{\mathrm{NN}}=0.5,\quad J_{\mathrm{NNN}}=0.07,\quad J_T=0.21,\quad K_P=0.29 \quad (75)$$

all in mK.

The magnetization of the "PF" phase obtained, within the coupled-cluster approximation by differentiating the energy [Eq. (50)] is shown in Fig. 15 (solid curve); it is compared to the molecular-field approximation (dotted line). At high field, $B/B_{c2}\approx 0.8$ there is a change of the magnetization curvature, which becomes negative in the neighborhood of B_{c2}. The mean-field approximation does not account for this important feature.

In Fig. 16, we compare the energies of the "PF" and "UUDD" phases at low field within the coupled-cluster approximation (solid lines). For the UUDD phase, the coupled-cluster approximation is applied in zero field. With S given by Eq. (74), the solution of the coupled-cluster equations (21) leads to

$$E_{\mathrm{UUDD}}/N=-1.07 \quad (76a)$$

in mK, with

TABLE III. The main exchange frequencies calculated by Monte Carlo methods from the first principles[6] (first column). The four largest are obtained with a reasonable accuracy. Large error bars subsist on the others. We have scaled them to melting molar volume, using a factor v[18] (second column).

Type of exchange	Exchange frequency (mK) at 24.12 cm^3/mol[6]	Exchange frequency (mK) scaled at 24.22 cm^3/mol
J_{NN}	0.46 (±7%)	0.495 (±7%)
J_{NNN}	0.065 (±10%)	0.07 (±10%)
J_T	0.19 (±10%)	0.205 (±10%)
K_P	0.27 (±10%)	0.29 (±10%)
K_F	0.027 (±18%)	0.03 (±18%)
S_1	0.036 (±30%)	0.039 (±30%)
S_2	0.022 (±35%)	0.024 (±35%)

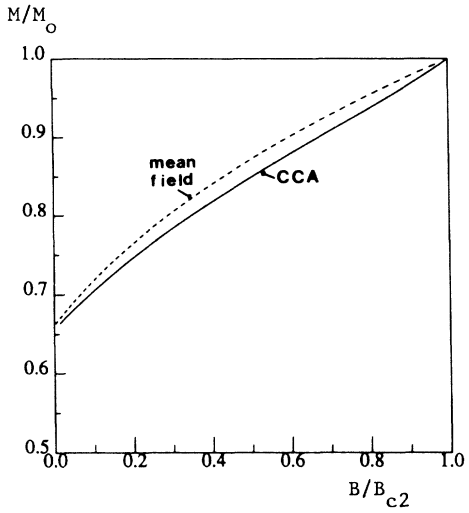

FIG. 15. The magnetization of the PF phase of bcc ^{3}He retaining only the most important exchange processes: $J_{NN}=0.50$ mK, $J_{NNN}=0.07$ mK, $J_T=0.21$ mK, and $K_P=0.29$ mK. B_{c2} is the critical transition field to the ferromagnetic state. The results of the coupled-cluster approximation (solid line) are compared to molecular field (dashed line).

$$\chi_1^a=0.1132,\quad \chi_2^a=-0.0366,\quad \chi_3^a=0.0090$$

and (76b)

$$\chi_1^b=\chi_2^b=\chi_3^b=\kappa_P^a=\kappa_P^b=0\ .$$

The last five coefficients are automatically zero: In zero field, as assumed here, the mean-field ground state is an eigenstate of the J_z operator. Since the Hamiltonian commutes with J_z it does not mix states with a different magnetic quantum number. The χ^b and κ_P terms in S all would mix in such states. (When $B\neq 0$ however the mean-field state is not an eigenstate of J_z and application of the Hamiltonian on that state can change the average magnetic quantum number.)

In a small magnetic field B a quadratic correction: $-\chi_{MF}B^2/2$, where

$$\chi_{MF}=[2(2J_{NN}+J_{NNN}-16J_T+12K_P)]^{-1} \tag{77}$$

represents the molecular-field susceptibility[3,8] is added to the energy.

For the PF phase, the coupled-cluster approximation is applied in arbitrary magnetic field. The solution has a completely different symmetry: all parameters in S are of the same order of magnitude. For example, at the transition field B_{c1} with the UUDD phase, we obtain

$$\chi_1=0.0583,\ \chi_2=-0.0158,\ \chi_3=-0.0077\ ,$$
$$\tau=-0.0121,\ \kappa_P=-0.0103 \tag{78}$$

and

$$\cos(\theta)=0.648\ .$$

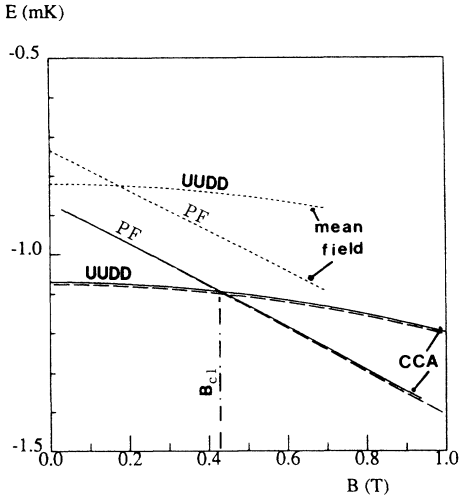

FIG. 16. The energies of the PF and UUDD phases at low field for the following set of exchange parameters: $J_{NN}=0.50$ mK, $J_{NNN}=0.07$ mK, $J_T=0.21$ mK, and $K_P=0.29$ mK. The coupled-cluster approximation (solid lines) is compared to the spin-wave approximation (dashed lines) and molecular field (dotted lines). The transition field between the two phases is B_{c1}.

For comparison, the energies of both phases have also been calculated by a spin-wave approximation and are shown in Fig. 16 (dashed lines). We use the relations D26–34 and D60–62 of Ref. 3. The summations over the first Brillouin zone are performed numerically using Gaussian quadrature. For both phases, the spin-wave results are very close to those obtained within CCA. We do not know the significance of this fact. This is not quite surprising for the UUDD phase where only quadratic terms finally remain in the CCA [when all possible pair flips are included, the spin-wave theory appears as some subset of the SUB2 CCA (Ref. 1)]. For the PF phase where higher-order terms contribute, such an agreement may suggest that both approximations are good when applied to the multiple-exchange Hamiltonian.

The dotted lines represent the mean-field approximation. The fluctuations are important with a correction of order 30% for the ground-state energy of the UUDD phase. The energy correction is lower for the PF phase and, consequently, the transition field B_{c1} (in T) between both phases is higher than the molecular-field value. We obtain within CCA

$$B_{c1}\approx 0.42\ \text{T}\ . \tag{79}$$

Although B_{c1} is in close agreement with the experimental data: 0.45 T, the second-order transition field to the ferromagnetic state

$$B_{c2}=8[J_{NN}+6(K_P-J_T)]\approx 10.1\ \text{T} \tag{80}$$

is only half of the experimental value $B_{c2}\approx 21$ T.[30]

As emphasized in Ref. 8, although small, higher-order ring exchanges (as six-spin exchange) play a significant role in the PF phase at high field and increase substantial-

ly the transition field B_{c2}. We shall take them into account in the following section.

3. *Corrections for smaller exchange processes; six-spin ring exchanges, etc.*

From Refs. 5 and 6, the next processes to take into account are six-spin ring exchanges and folded four-spin exchange (K_F). Two kinds of six-spin exchange cycles have a significant contribution (see Refs. 6, 8, and Fig. 13), we shall keep the notations of Ref. 8: S_1 and S_2. The relevant parameter for six-spin exchanges in mean-field equations is, in fact,

$$S_{ix}=S_1+3S_2 \ . \tag{81}$$

From Table III, the values of these parameters, scaled at melting molar volume $v=24.22$ cm^3/mol are

$$K_F=0.03\pm0.006 \text{ mK}$$

and (82)

$$S_{ix}=0.11\pm0.04 \text{ mK} \ .$$

Since the Monte Carlo calculation of S_{ix} is still inaccurate, we shall allow some readjustment of this parameter within the error bar given by Ceperley and co-workers [see Eq. (82)].

The exact value of the transition field B_{c2} to the ferromagnetic state is[8]

$$B_{c2}=8[J_{\rm NN}+6(K_P+K_F+S_{ix}-J_T)] \ . \tag{83}$$

Taking S_{ix} at the upper limit of the error bar: $S_{ix}=0.15$ mK, we obtain $B_{c2}=21.2$ T, in good agreement with the experimental value.[30] Hence, we use the following set of exchange frequencies:

$$J_{\rm NN}=0.50 \text{ mK}, \ J_{\rm NNN}=0.07 \text{ mK}, \ J_T=0.21 \text{ mK} \ , \tag{84}$$

$$K_P=0.29 \text{ mK}, \ K_F=0.03 \text{ mK}, \ S_{ix}=0.15 \text{ mK} \ .$$

We now apply the coupled-cluster method, with the following approximation: we only keep the lowest-order terms in the small parameters K_P, S_1, and S_2 (≈ 0.03 mK, see Table III), and neglect higher-order terms like $K_P\chi_n$, $K_P\kappa$, $S_1\chi_n$, $S_1\kappa$, $S_2\chi_n$, and $S_2\kappa$, ... The contributions of folded four-spin and six-spin exchanges to the ground-state energy are thus the same as their contribution to the mean-field energy:[8]

$$\Delta E_{\rm PF}=-3K_F/2-S_{ix}/4+12K_F m^4+8S_{ix}m^6 \tag{85}$$

for the PF phase, where m is the magnetization $m=\cos(\theta)$. For the UUDD phase,

$$\Delta E_{\rm UUDD}=K_F/2-S_{ix}/4 \ . \tag{86}$$

For the PF phase, the contribution to the first coupled-cluster equation with one spin flip is

$$\langle 0|\sigma_i^-(\Delta\tilde{H})|0\rangle=\frac{\partial \Delta E_{\rm PF}}{\partial\theta}$$
$$=-\sin(\theta)[48K_F\cos^3(\theta)+48S_{ix}\cos^5(\theta)] \tag{87}$$

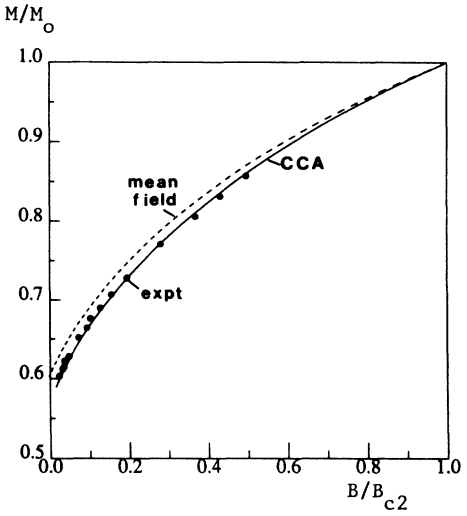

FIG. 17. The magnetization of the PF phase of bcc ^{3}He, with corrections due to six-spin ring exchanges and folded four-spin ring exchange. The exchange parameters are: $J_{\rm NN}=0.50$ mK, $J_{\rm NNN}=0.07$ mK, $J_T=0.21$ mK, $K_P=0.29$ mK, $K_F=0.03$ mK, and $S_{ix}=S_1+3S_2=0.15$ mK. The coupled-cluster approximation (solid curve) is compared to the experimental data[30] (●). The molecular-field approximation (dashed line) is also shown.

as can be seen from Eq. (9).

The magnetization curve thus obtained for the PF phase is represented in Fig. 17 (solid curve) and compared to the experimental results. The agreement is excellent.

The energies of both phases at low field are plotted in Fig. 18. For the UUDD phase, a correction $-\chi_{\rm MF}B^2/2$ is added to the zero-field energy (cf. preceding subsection) with:[8]

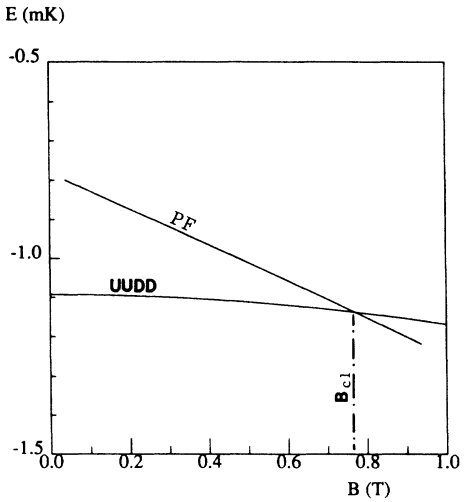

FIG. 18. Energies of the PF and UUDD phases, within coupled-cluster approximation with corrections due to six-spin ring exchanges. The exchange parameters are the same as for Fig. 17. The transition field becomes: $B_{c1}\approx 0.76$ T.

$$\chi_{MF}=[2(2J_{NN}+J_{NNN}-16J_T+12K_P+8K_F+4S_{ix})]^{-1} \approx(4.06\ \text{mK})^{-1} \quad (88)$$

This molecular-field susceptibility is in close agreement with the experimental value:[30] $(3.84\ \text{mK})^{-1}$. Godfrin and co-workers[8] claim that the molecular-field susceptibility should be reduced approximately 20% by the fluctuations. This is true for a Heisenberg model, but this does not seem quite obvious to us for ring exchange Hamiltonians. Four-spin exchange enhances the susceptibility so that in the paramagnetic phase, in contrast to the Heisenberg model, the susceptibility is higher than the mean-field estimate.[24,28] This latter effect might compensate the former.

The energy of the UUDD phase at zero field is $E_{UUDD}\approx -1.095$ mK. It is in agreement with the experimental value $E_{UUDD}\approx -1.24$ mK, obtained by Fukuyama and co-workers[31] if one takes into account the error bars on the exchange frequencies (10%) (Ref. 6) and on the coupled cluster approximation (a few percent).

The transition field $B_{c1}\approx 0.76$ T between the UUDD and PF phase is higher than the experimental value: 0.45 T. This difference is compatible with the errors bars on the exchange parameters. Note that other smaller exchange processes that we have neglected might lower this calculated transition field.[8]

4. *Relation to finite temperature phase diagram and other measured quantities*

We finally emphasize that the set of exchange frequencies represented by the relation (84) is compatible with all other thermodynamic data on bcc ^{3}He. For example, the Curie Weiss temperature

$$\Theta=-[4J_{NN}+3J_{NNN}+18(K_P+K_F-2J_T)+15S_{ix}/2] \approx -1.54\ \text{mK} \quad (89)$$

is in agreement with experimental data:[32] $\Theta\approx -1.8\pm 0.2$ mK. A rough estimate of the critical temperature T_{c1} for the first-order transition at zero field from the UUDD to the paramagnetic phase is[3]

$$T_{c1}=-E^{MF}_{UUDD}/\ln(2)\ , \quad (90)$$

where

$$E^{MF}_{UUDD}=J_{NNN}/2-2J_T-3K_P/2+K_F/2-S_{ix}/4 \approx -0.842\ \text{mK} \quad (91)$$

represents the mean-field energy[8] of the UUDD phase. We obtain $T_{c1}\approx 1.2$ mK in a reasonable agreement with the experimental value ≈ 0.92 mK.[31]

The second-order critical transition temperature of the NAF phase to the paramagnetic phase is

$$T_{c2}=4J_{NN}-3J_{NNN}-12J_T+6(K_F+K_P)+3S_{ix}/2 \approx 1.4\ \text{mK} \quad (92)$$

a value close to T_{c1}. In a more realistic approximation,[33] it would probably move below T_{c1}, in agreement with the experimental results.[3,4]

Other smaller exchange parameters have been taken into account in Ref. 8. In contrast to six-spin ring exchanges, their effects are weak. However, since the energy difference between the UUDD and PF phase is very small, they might affect substantially the transition field.

We have chosen the six-spin exchange parameter S_{ix} at the upper limit of Ceperley's error bars to account for the experimental transition field H_{c2} of order 21 T. As pointed out by Godfrin and Osheroff,[8] higher-order ring exchanges, although exponentially decreasing, might give a significant contribution to H_{c2}. In that case, the experimental data could be interpreted with a lower S_{ix} and some small eight-spin exchange. Unfortunately, the precision of the Monte Carlo calculations for high-order (six and eight spin) ring exchanges is poor.

We think that it is reasonable to wait for more accurate Monte Carlo calculations of all of these small exchange parameters [some of them such as the rigid rotation of a compact four-particle tetrahedron (cf. Fig. 13 of Ref. 2) remain to be investigated] before taking them into account. We could then apply the coupled-cluster approximation in a completely consistent way, including all exchange processes.

5. *Predictions for the variations of B_{c1}/B_{c2} in terms of the molar volume*

Most experiments on bcc ^{3}He magnetism have been performed at the melting molar volume. A few experimental studies[34,35] at lower molar volume have shown that most physical quantities (critical temperature T_{c1}, coefficients of high-temperature series expansions, susceptibility...) simply scale as v^γ with $\gamma=18\pm 2$ (this somewhat surprising result is also obtained from exchange-frequency variations calculated from first principles[5]). The physical parameter which is the most sensitive to small variations of the ratios between various exchange frequencies is precisely the transition field B_{c1} between the two almost degenerated UUDD and PF phases. It is interesting to predict, at least qualitatively, its variation as a function of the molar volume.

The variations of the exchange frequencies with molar volume have been predicted within a multidimensional WKB approximation.[5] We have

$$J_P\approx C_P s_P \exp(-A_P/g)\ . \quad (93)$$

The dimensionless action A_P for various exchange frequencies is given in Table IV. The symmetry factor s_P represents the number of equivalent exchange channels in the $3N$-dimensional configuration space: $s_P=12$ for pair exchange between first neighbors, $s_P=8$ for pair exchange between second neighbors and $s_P=1$ for all other ring exchanges considered. C_P is a prefactor which varies slowly as a function of density. The variation with density enters through the parameter g,

$$g=\frac{\hbar}{[8m\sigma^{*2}\epsilon]^{1/2}}\left[\frac{a}{\sigma^*}\right]^5\ , \quad (94)$$

which varies strongly with the first neighbor distance a. Also in Eq. (94) m represents the mass of a ^{3}He atom,

TABLE IV. Action A_P and symmetry factor s_P [cf. Eqs. (93) and (94)] within a multidimensional WKB approximation (Ref. 5). In spite of its relatively large action, J_{NN} is favored by its large symmetry factor.

	J_{NN}	J_T	K_P	K_F	S_1
WKB action[5]	10.2	9.09	8.47	10.13	10.58
Symmetry factor	12	1	1	1	1

$\epsilon=10.22$ K and $\sigma^*=0.265$ nm are the parameters of an effective pair potential $\epsilon(\sigma^*/a)^{12}$ which were determined to account for the variations of the macroscopic elastic quantities pressure and compressibility (see Ref. 4, Sec. IV).

Although the applicability of this approximation at the physical densities of bcc ^{3}He, has been severely questioned,[4] the Monte Carlo calculations[6] have remarkably confirmed its predictions. Figure 19 shows a plot of $\ln(J_P^{(MC)}/s_P)$, $J_P^{(MC)}$ representing the Monte Carlo value of various exchange parameters at 24.12 cm^{3}mol (Refs. 6 and 36) (see Table III) as a function of the corresponding action A_P within WKB calculation [cf. Eq. (93) and Table IV]. All points are roughly aligned on a straight line of slope $-1/g\approx-1.1$, which represents the Eqs. (93) and (94) with the theoretical value of g at $v=24.12$ cm^3/mol. The dispersion around this line is compatible with the differences in various C_P prefactors.

As first emphasized in Ref. 5, the fact that J_{NN} is of the same order of magnitude as K_P is due to its important symmetry factor $s_P=12$, its action A_P being larger and comparable to the action for six-spin exchange. As a consequence, when the density increases, J_{NN} is expected to decrease faster than K_P. This has an important consequence: Since J_{NN} favors the PF phase with respect to the UUDD phase, the transition field B_{c1} should increase when the density increases.

Using Eqs. (93) and (94) with Table IV and the values of J_P at 24.12 cm^3/mol given by Ceperley *et al.*, we predict

$$J_T/J_{NN}\approx0.64,\ K_P/J_{NN}\approx1.15,\ S_{ix}/J_{NN}\approx0.34 \quad (95)$$

at 20.07 cm^3/mol. Note that these predictions differ from the values given, somewhat tentatively (the precision is poor) by Ceperley *et al.* at this low molar volume. Ceperley's values,

$$J_T/J_{NN}\approx0.27,\ K_P/J_{NN}\approx0.40\ , \quad (96)$$

rather suggest an enhancement of J_{NN} with respect to K_P, and, in that case the transition field B_{c1} should decrease and eventually the UUDD phase should disappear.

Using the method of the preceding subsection (see Fig. 18), and with the exchange frequencies given by Eq. (95), we predict $B_{c1}/B_{c2}\approx0.055$ at $v=20.07$ cm^3/mol, which is to be compared with the theoretical value $B_{c1}/B_{c2}\approx0.036$ at melting molar volume. Similar calculations have been done at a few intermediate volumes. Figure 20 shows the variations of the ratio between the two transition fields: $\xi(v)=B_{c1}/B_{c2}$ as a function of the molar volume. This curve should only be considered as semiquantitative: at melting density, the calculated value $\xi\approx0.036$ differs substantially from the experimental one $\xi\approx0.0215$. However the predicted derivative

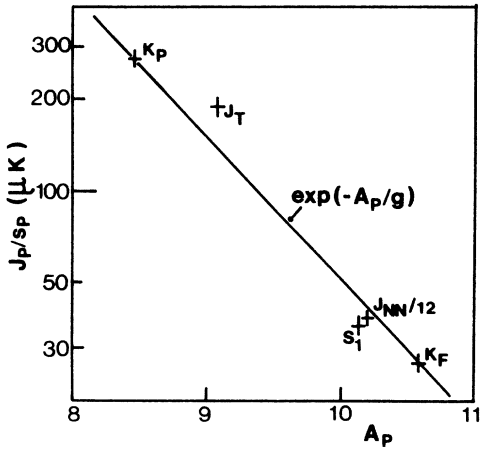

FIG. 19. Semi-log plot of the Monte Carlo values J_P of the exchange frequencies,[6] divided by the respective symmetry factors s_P, as a function of the WKB approximation[5] for the action A_P. The straight line represents the Eqs. (93) and (94), with slope $-1/g\approx-1.1$, calculated at $v=24.12$ cm^3/mol. Both calculations are in remarkable agreement.

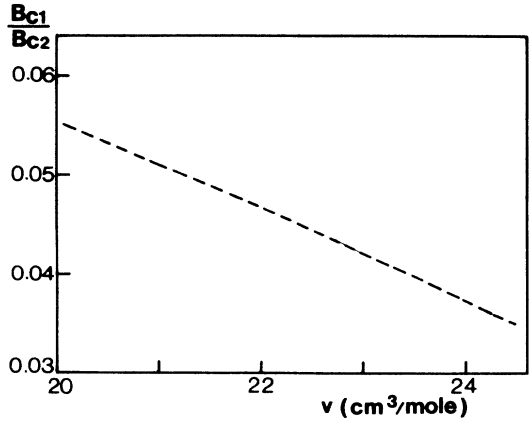

FIG. 20. Predicted variations of the ratio of the transition fields $\xi=B_{c1}/B_{c2}$ as a function of molar volume.

$$\frac{\partial \xi}{\partial v} \approx -4.4 \times 10^{-3} \tag{97}$$

in cm^{-3} should be more accurate.

V. CONCLUSION

We have extended the coupled-cluster approximation to the spin-lattice problem and proven that it works quite well for various quantum-spin Hamiltonians from the Heisenberg model to more complicated systems with quartic interactions. We have predicted some interesting properties of the magnetization for a two-dimensional square lattice of ^{3}He adsorbed on an appropriate substrate.

Using the exchange parameters determined from the first principles,[5,6] we have calculated the transition field between the two ordered phases of bcc ^{3}He and predicted its variations in terms of the molar volume. At melting density, the best estimate of this critical field is a factor 1.7 too large but within the large theoretical error bars on the exchange frequencies is consistent with the experiments. The magnetization curve of the high field phase fully agrees with experimental results. The agreement with other experimental data at finite temperature is also noted. In spite of the skepticism expressed by some authors,[4] solid ^{3}He might be one of the rare quantum many-body systems where all magnetic properties can be quantitatively interpreted, starting from the Schrödinger equation.

ACKNOWLEDGMENTS

Part of this work was motivated by exciting discussions with Hiroshi Fukuyama and Hidehiko Ishimoto on the possibility of measuring the critical fields in bcc ^{3}He at higher densities and very low temperatures. One of the authors (J.H.H.) wishes to thank the "Commissariat à l'Energie Atomique" (91191 Gif-sur-Yvette, France) for its hospitality.

APPENDIX

We present here a short description of the method used to mechanize the computation of a product of n operators $\tilde{\sigma}_i^{\lambda}$ summed over a given lattice.

We start from the relations (26,27) of Sec. II:

$$\tilde{\sigma}_i^{+} = \sigma_i^{+} , \tag{26a}$$

$$\tilde{\sigma}_i^{-} = \sigma_i^{-} + [\sigma_i^{-}, \sigma_i^{+}]\mathcal{S}_i - \sigma_i^{+}\mathcal{S}_i^2 , \tag{26b}$$

$$\tilde{\sigma}_i^{z} = [\sigma_i^{+}, \sigma_i^{-}] + 2\sigma_i^{+}\mathcal{S}_i , \tag{26c}$$

where $\sigma_i^{+}\mathcal{S}_i$ represents the sum of all terms of S which are connected to the site i (i.e., which contain σ_i^{+}).

$$\mathcal{S}_i = \sum_{P_2^i} \sum_{j}^{(P_2^i)} \chi_{ij}\sigma_j^{+} + \sum_{P_3^i} \sum_{j<k}^{(P_3^i)} \tau_{ijk}\sigma_j^{+}\sigma_k^{+} + \sum_{P_4^i} \sum_{j<k<l}^{(P_4^i)} \kappa_{ijkl}\sigma_j^{+}\sigma_k^{+}\sigma_l^{+} + \cdots . \tag{27}$$

The sums are restricted to the panels P_n^i connected to i

As shown in Sec. II, the expression of $\tilde{H}|0\rangle$ can be reduced to a sum of terms like

$$G^{(P_n)}_{\rho\tau\mu\nu\cdots}\,\tilde{\sigma}_i^{\rho}\tilde{\sigma}_j^{\tau}\tilde{\sigma}_k^{\mu}\tilde{\sigma}_l^{\nu}\cdots|0\rangle .$$

We have written a computer program to calculate any given product having this form with $i,j,k,l\ldots$ fixed. In the following description, the fixed sites will be renamed $i_0, j_0, k_0, l_0, \ldots$, other indices will represent free sites connected to the fixed sites through $\mathcal{S}$.

We have to substitute one of the expressions [26(a)–(c)] to $\tilde{\sigma}_{m_0}^{\alpha}$ at each site, expand the product and reduce each of the elementary σ_p^{λ} operator products thus obtained ($\lambda = \pm$), taking into account the commutation rules (12–15). (The σ_p^{-} operators can be moved to the right and eliminated since $\sigma_p^{-}|0\rangle = 0$ and we are left with products of raising operators σ_p^{+}). Note that this may lead to a huge number of terms. To fix the ideas, consider a product of four operators $\tilde{\sigma}_{m_0}^{-}$ in the bcc phase of ^{3}He where $\mathcal{S}$ contains about 100 different terms. Each $\tilde{\sigma}_{m_0}^{-}$ contains $\mathcal{S}^2$, i.e., 10^4 terms and the expanded product involves 10^{16} elementary products. Fortunately, most of them vanish, due to the fact that all σ_p^{+} commute and $(\sigma_p^{+})^2 = 0$.

To avoid the impossible task complete construction of the 10^{16} terms, we have to write an algorithm which stops the construction of a given set of terms as soon as two σ_p^{+} operators are found on the same free site p different from $i_0, j_0, k_0, l_0 \ldots$. Lowering operators $\sigma_{m_0}^{-}$ do not commute with the $\sigma_{m_0}^{+}$, however, they only occur on fixed sites $i_0, j_0, k_0, l_0 \ldots$ and these are treated separately.

The essential part of the algorithm is a short subroutine which is used to reduce the operator products applied to $|0\rangle$ as they are constructed and returns as soon as it detects two raising operators on the same free site. Such operator product is specified by the state s_{m_0} of each of the fixed sites $i_0, j_0, k_0, l_0 \ldots$ which is 1 for a raising operator σ_p^{+} occurring on that site and 0 otherwise, and by the labels on the lattice of the free sites corresponding to the other σ_p^{+} operators ($p \neq i_0, j_0, k_0, l_0 \ldots$) which are present. The key subroutine performs the following task. It multiplies a given product by a new operator σ_n^{λ} on the left and determines the new product or returns if the result is zero. (i) If n is a free site ($n \neq i_0, j_0, k_0, l_0 \ldots$) the subroutine compares the new label n to all the labels of raising operators already contained in the previous product; if it matches with one of them the result is zero, otherwise the subroutine stores the new label n. (ii) If n is one of the fixed sites $i_0, j_0, k_0, l_0, \ldots$, the state s_n is changed with the simple following rules: (a) if $\lambda = +$, the result is zero if $s_n = 1$, otherwise s_n is changed from 0 to 1, and (b) if $\lambda = -$, the result is zero if $s_n = 0$ (since σ_n^{-} commutes with all operators on other sites, it can be moved to the right and $\sigma_n^{-}|0\rangle = 0$); otherwise s_n is changed from 1 to 0 [we use the relation (15): $\sigma_n^{-}\sigma_n^{+} = 1 - \sigma_n^{+}\sigma_n^{-}$, and the second term obviously does not contribute].

In this algorithm, most terms are eliminated from the first steps of the factor expansion and the calculation becomes feasible. The total amount of time needed for the PF phase of bcc ^{3}He was about one CPU hour on Convex C1 computer at Saclay. This CPU time could have been

reduced by taking into account the symmetries on the lattice. However, we did not take advantage of this saving so as to avoid complications and sources of errors in programming.

The coupled-cluster equations are directly written by the program in algebraic literal form. Then these equations are solved by the Newton-Raphson program MNEWT of Ref. 12.

[1]R. F. Bishop and H. G. Kümmel, Phys. Today **40**(3), 52 (1987), and references therein.

[2]J. M. Delrieu, M. Roger, and J. H. Hetherington, J. Low Temp. Phys. **40**, 71 (1980).

[3]M. Roger, J. H. Hetherington, and J. M. Delrieu, Rev. Mod. Phys. **55**, 1 (1983).

[4]M. C. Cross and D. S. Fisher, Rev. Mod. Phys. **57**, 881 (1985).

[5]M. Roger, Phys. Rev. B **30**, 6432 (1984).

[6]D. M. Ceperley and G. Jacucci, Phys. Rev. Lett. **58**, 1648 (1987).

[7]H. Stipdonk and J. H. Hetherington, Phys. Rev. B **31**, 4684 (1985).

[8]H. Godfrin and D. D. Osheroff, Phys. Rev. B **38**, 4492 (1988).

[9]M. C. Cross and R. N. Bhatt, Phys. Rev. B **33**, 7809 (1986).

[10]M. Roger, Ph.D. thesis, University of Paris–Sud, 1980.

[11]K. Iwahashi, Y. Miwa, and Y. Masuda, J. Phys. Soc. Jpn. **53**, 3088 (1984).

[12]W. H. Press, B. P. Flannery, S. A. Teukolsky, and W. T. Vetterling, *Numerical Recipes* (Cambridge University Press, New York, 1986).

[13]P. W. Anderson, Phys. Rev. **86**, 694 (1952).

[14]L. Hulthén, Arkiv. Mat. Astron. Fys. **26A**, 1 (1938).

[15]P. W. Anderson, Mater. Res. Bull. **8**, 153 (1973).

[16]D. A. Huse and V. Helser, Phys. Rev. Lett. **60**, 2531 (1988).

[17]R. B. Griffiths, Phys. Rev. **133A**, 768 (1964).

[18]C. K. Majumdar, J. Phys. C **3**, 911 (1970).

[19]T. Tonegawa and I. Harada, J. Phys. Soc. Jpn. **56**, 2153 (1987).

[20]D. J. Thouless, Proc. R. Phys. Soc. London **86**, 893 (1965).

[21]H. Godfrin, R. R. Ruel, and D. D. Osheroff, Phys. Rev. Lett. **60**, 305 (1988).

[22]M. Roger and J. M. Delrieu, Jpn. J. Appl. Phys. **26**, Suppl. 26-3, 267 (1987); M. Roger (to be published).

[23]R. F. Buzerak and R. J. Rollefson, J. Low Temp. Phys. **38**, 105 (1980).

[24]M. Roger and J. M. Delrieu, Phys. Rev. B **39**, 2299 (1989).

[25]J. Oitmaa and D. D. Betts, Can. J. Phys. **56**, 897 (1978).

[26]T. Oguchi, H. Nishimori, and Y. Taguchi, J. Phys. Soc. Jpn. **55**, 323 (1986).

[27]We use an efficient variant of the Lanczös method proposed by E. R. Gagliano, E. Dagotto, A. Moreo, and F. C. Alcaraz, Phys. Rev. B **34**, 1677 (1986).

[28]M. Roger, E. Suaudeau, and M. E. R. Bernier, Phys. Rev. B **35**, 2091 (1987).

[29]A. Benoit, J. Bossy, J. Flouquet, and J. Schweizer, J. Phys. (Paris) Lett. **46**, L-923 (1985).

[30]D. D. Osheroff, H. Godfrin, and R. R. Ruel, Phys. Rev. Lett. **58**, 2458 (1987).

[31]H. Fukuyama, H. Ishimoto, T. Tazaki, and S. Ogawa, Phys. Rev. B **36**, 8921 (1987).

[32]W. P. Kirk, Z. Oleiniczak, P. Kobiela, A. A. V. Gibson, and A. Czernmak, Phys. Rev. Lett. **51**, 2128 (1983).

[33]J. H. Hetherington, J. Low Temp. Phys. **66**, 145 (1987).

[34]T. Mamiya, A. Sawada, H. Fukuyama, Y. Hiro, and Y. Masuda, Phys. Rev. Lett. **47**, 1304 (1981).

[35]Y. Miura, N. Nishida, Y. Takano, H. Fukuyama, H. Ishimoto, and S. Ogawa, Phys. Rev. Lett. **58**, 381 (1987).

[36]D. M. Ceperley pointed out to us the relevance of such a plot.